A STEP TOWARDS LANDMINE DETECTION: MEASUREMENTS OF 2,4-DINITROTOLUENE SOIL SURFACE FLUX FROM A BURIED POINT SOURCE

by

Matthew J. Gozdor

Submitted in Partial Fulfillment of the Requirements for the

Master of Science in Hydrology

New Mexico Institute of Mining and Technology

Department of Earth and Environmental Science

Socorro, New Mexico

December, 2000

ABSTRACT

Anti-personnel devices, commonly known as landmines, are a danger to both the military and civilians. Current landmine detection techniques are inadequate, as they often produce false positive and false negative results. The research presented here is a first step toward determining the chemical signature, or surface vapor flux from a simulated landmine under steady state and variable boundary conditions. The results from this thesis will be combined with computer simulations being conducted at Sandia National Laboratories and other detection techniques to create an integrated sensor that will improve landmine detection technology.

Two laboratory experiments were conducted on a packed soil column (15-cm diameter, 32-cm length) under steady state and varying boundary conditions to determine the surface vapor flux of 2,4-dinitrotoluene (2,4-DNT) from a point source. An aqueous solution of 2,4-DNT (~150 mg/L) was introduced via a syringe through a polytetrafluoroethylene (PTFE) mininert valve inserted approximately 3 cm from the top of the column. Volumetric water content was measured along the length of the column by five water content reflectometers (WCR). The surface vapor flux was determined using a solid phase microextracion fiber (SPME) placed near the center of a sweep-air plenum attached to the top of the column.

During the first experiment, the relative humidity and volumetric flow rate of the sweep gas and the matric potential in the soil remained essentially constant, and the 2,4-DNT surface flux approached steady state: approximately 70,000 pg 2,4-DNT/min over a period of 29 days. The second experiment initially employed the same boundary conditions, producing nearly identical results and surface fluxes. The second experiment was then appended with an increased evaporation phase, a drying phase, and two wetting phases. Once the soil water content was decreased approximately to 8% volumetric, the soil surface flux of 2,4-DNT decreased four orders of magnitude from 275,000 pg/min to 70 pg/min over 25 days. Two simulated rainfall events produced 2,4-DNT surface fluxes that rose 3 orders of magnitude, from approximately 70 pg/min to 70,000 pg/min over the course of a few hours. This data suggests the optimum window to search for the chemical signature of a landmine would be the period shortly after a rainfall, immediately preceded by drying conditions.

ACKNOWLEDGMENTS

I would like to thank the members of my advisory committee, namely Drs. Rob Bowman, Mark Cal, and Jan Hendrickx. Without their advice, help, and expertise this effort would not have been possible. Further thanks are due to James Phelan and Stephen W. Webb of Sandia National Labs who gave us the funding for this project and who conducted some related experiments and computer simulations for this project.

Without my friends Ben Moayyad and Alana Fuierer, I'm not sure I would have made it through "life in Socorro". Your abilities to make me realize what is really important never cease to amaze me. Thank you very much for all the help you have given me.

While everyone heretofore mentioned has contributed to this project in some direct or physical way, there is one very special person who rarely understands me when I discuss the contents of this thesis: my wife Rebecca Gozdor. I owe an enormous debt to her as she conceded to me living 2,000 miles away, so I could obtain my Master of Science. Her faith in our relationship and in me was unprecedented during this period. To her, I dedicate this paper.

TABLE OF CONTENTS

Page

LIST OF FIGURES

Figure Page

LIST OF TABLES

Table Page

1. INTRODUCTION AND PROBLEM STATEMENT

In the last century, the use of landmines has proliferated around the world. Landmines have caused serious injury and death not only to military personnel, but also to innocent civilians. Currently, it is estimated that there are approximately 100 million mines deployed worldwide, and at current removal rates, it will take approximately 1,000 years to remove those mines (Phelan et al., 1999). As a result of the numbers of mines and the threat of destruction they impose, it has become necessary to be able to detect buried landmines.

Presently the only successful means of de-mining an area is to use humans or dogs. Both of these methods are currently unacceptable due to high casualty rates. There are several other techniques being investigated which revolve around the idea of unexploded ordnance reflecting electromagnetic signals (Borchers et al., 2000). These methods often result in both false positive and false negative results as many objects are capable of reflecting electromagnetic radiation (i.e. bayonets, grenades, bomb fragments, etc.) (Phelan et al. 1999)

In light of current shortcomings in landmine detection, it becomes clear that to detect landmines it is necessary to try to detect something that is unique to the mine regardless of its environment. With mines being composed of charges consisting of explosive

organic compounds, the most obvious choice is a chemical signature as long as the environment was not previously contaminated with explosive compounds. Before sensing landmines as a result of their chemical signatures, it is necessary to determine the surface flux of the chemicals under various environmental conditions. Quantifying this surface flux is the overall intent of this research.

Other researchers have presented results concerning the surface flux of a chemical applied to a soil (Spencer and Cliath, 1973; Jury et al., 1983, 1984 a,b,c; Peterson et al.,1996). These experiments were all conducted in a manner similar to the experiments that will be presented in this thesis. However, no previous work has been completed regarding the surface flux behavior of 2,4-DNT, nor has any work attempted to examine the surface flux of a chemical under variable top and bottom boundary conditions. This thesis will specifically examine these details.

1.1. Goals

The intent of this study was to use an instrumented unsaturated soil column to be able to quantify the surface vapor flux of explosives commonly found in anti-personnel devices. Specifically, it was necessary to gain a greater understanding of the emissions of a buried point source of 2,4-dinitrotoluene (2,4-DNT) from a soil surface under both steady state and variable boundary conditions. 2,4-DNT was chosen as it is a component of many American and Yugoslavian mines. In addition, 2,4-DNT is also the chemical that most frequently leaks from these mines (Phelan, 1999). Once these laboratory experiments were completed, the data were compared with the modeling efforts of researchers at

Sandia National Laboratories. After the model calibration is complete, the model will be employed to predict the chemical signature of landmines in various climatic conditions around the world. This will provide engineers with the data they need to design a chemical sensor capable of detecting landmines.

To this end, the following objectives were achieved. The results are presented in this thesis:

1) Measurement of soil properties which control the fate and transport of 2,4-DNT
2) Design and construction of a soil column suitable to the requirements of this research
3) Development of a water content reflectometer (WCR) calibration protocol
4) Development of a head space sampling protocol incorporating the use of solid phase microextraction fibers (SPME)
5) Analysis of the surface vapor flux of 2,4-DNT under steady state, wetting, and drying soil conditions
6) Analysis of 2,4-DNT soil concentrations at the conclusion of the experiments
7) Analysis of soil moisture content during the experiments and at their conclusion

2. THEORY: PHASE PARTITIONING RELATIONSHIPS

The location of 2,4-DNT in an unsaturated soil and its resulting flux from the soil surface is of prime interest to this research. As it is an organic contaminant, it can be found in one of four locations: sorbed onto soil particles, dissolved in the aqueous phase, partitioned into the gas phase, or in the free phase as a solid or liquid. Jury et al. (1983) have described this situation under equilibrium conditions with the following equation:

$$C_T = \rho_s C_s + \theta C_l + a C_g \qquad [2.1]$$

C_T is the total concentration of contaminant in the bulk soil. C_s, C_g, and C_l represent the concentrations in the solid, gas, and liquid phases. ρ_s is the dry bulk density of the solid phase, θ is the volumetric water content, and *a* is the volumetric air content. Jury et al. (1983) showed how equation [2.1] can be rewritten in terms of one of these variables:

$$C_T = R_s C_s = R_l C_l = R_g C_g \qquad [2.2]$$

where

$$R_s = \rho_s + \frac{\theta}{K_d} + a\frac{K_h}{K_d} \qquad [2.3]$$

$$R_l = \rho_s K_d + \theta + a K_h \qquad [2.4]$$

$$R_g = \rho_s \frac{K_d}{K_h} + \frac{\theta}{K_h} + a \qquad [2.5]$$

R_s, R_l, and R_g are the solid, liquid, and gas phase partition coefficients, respectively, which give the ratio of total contaminant concentration to the contaminant concentration in each respective phase. K_h is the Henry's Law constant $\left(K_h = \frac{C_g}{C_l} \right)$ and K_d is the solid-liquid partitioning coefficient $\left(K_d = \frac{C_s}{C_l} \right)$.

Jury et al. (1983) assume that the water content does not change. Furthermore, as the water content approaches zero, there is no provision for vapor-solid partitioning; only terms for gas-liquid (K_h) and solid-liquid (K_d) partitioning are present in the formulations of Jury et al. (1983). It was therefore necessary to develop partitioning relationships that include vapor-solid partitioning.

Work by Ong et al. (1991a,b, 1992) added the vapor-solid partitioning relationship, so that equations 2.1 and 2.2 become:

$$C_T = \theta C_l + a C_g + C_l K_d \rho_s + C_g K_{sg} \rho_s \qquad [2.6]$$

And

$$C_T = R_l C_l = R_g C_g = R_{sl} C_{sl} = R_{sg} C_{sg} \qquad [2.7]$$

Where

$$R_l = \rho_b K_d + \theta + a K_h + \rho_b K_h K_{sg} \qquad [2.8]$$

$$R_g = \rho_s \frac{K_d}{K_h} + \frac{\theta}{K_h} + a + \rho_s K_{sg} \qquad [2.9]$$

$$R_{sl} = \rho_s + \frac{\theta}{K_d} + a\frac{K_h}{K_d} + \frac{\rho_s K_h K_{sg}}{K_d} \qquad [2.10]$$

$$R_{sg} = \frac{\rho_s K_d}{K_h K_{sg}} + \frac{\theta}{K_h K_{sg}} + \frac{a}{K_{sg}} + \rho_s \qquad [2.11]$$

are the liquid, gas, solid-liquid, and solid-gas phase partition coefficients which, again, give the ratio of the total concentration of a contaminant to its concentration in each representative phase.. However Ong's formulation introduces a new term: K_{sg}. This term is a function of overall vapor solid partition coefficient (K_d'). K_d' is strongly dependent on soil moisture content. K_{sg} is defined as follows:

$$K_{sg} = K_d'(\omega) - \frac{K_d}{K_h} + \frac{\omega}{100 K_h \gamma \rho_w} \qquad [2.12]$$

where

$$K_d'(\omega) = \frac{K_d}{K_h} + \frac{\omega}{(K_h \gamma \rho_w)} \qquad [2.13]$$

and ω is gravimetric water content, γ is the aqueous activity coefficient ($\cong 1$), and ρ_w is the density of water.

These relationships (Eqns. 2.6-2.13) were verified for trichloroethylene (TCE) through experiments by Ong et al. (1991a) for water contents only greater than approximately 4 monomolecular layers of water. Ong et al. (1991a,b, 1992) found the values of K_d' at soil moisture contents greater than 4 monomolecular layers of water ($\omega>4$) were nearly constant and fell on the line predicted by Eqn 2.13. Peterson et al. (1994, 1995, 1996)

have conducted experiments with TCE that demonstrated the high degree of sorption of low vapor pressure organic compounds onto soil particles at water contents less than 4 monomolecular layers of water (ω<4). Furthermore, Peterson et al. (1995) were able to define an empirical relationship to describe the non-linear behavior of K_d' as a function of water content from oven-dry to saturated soil conditions.

$$A = \log(K_d'(\omega)) \qquad [2.14]$$

$$A = (A_0 - \beta(\omega))e^{-\alpha\omega} + \beta(\omega) \qquad [2.15]$$

$$\beta(\omega) = \log\left(\frac{K_d}{K_h} + \frac{\omega}{K_h \gamma \rho_l}\right) \qquad [2.16]$$

A_o is the K_d' value at zero moisture content. Alpha is a fitting parameter that describes the curvature of the nonlinear portion of the curve. The first term of equation [2.15] describes the non-linear region and the second term describes the linear region of the curve. Therefore the gravimetric water content at which the curve became linear (ω>4) describes the threshold at which Henry's Law becomes important to the concentration of a volatile organic compound in the gas phase.

Ong et al. (1991a,b, 1992) and Peterson et al. (1996) both report a reason for transition of high to low values of K_d' when soil moisture content goes from the dry region (ω<4) to the wet region (ω>4). Water is more polar than many organic compounds. Thus, as more water becomes available to cover the soil surface, it essentially out-competes the organic contaminant for sorption sites on the soil surface. Therefore, less of the organic compound is able to adsorb onto the soil surface and more will be available to partition into the gas phase.

Applying the results of Ong et al. (1991a,b, 1992) and Peterson et al. (1994, 1995, 1996) to the problem of landmine detection is necessary. The concentration of 2,4-DNT in the gas phase is the limiting factor in detecting the chemical signature of a landmine. The partitioning relationships then are critical in determining how much 2,4-DNT will be able to escape from the bulk soil. In short the relationships presented in this section, along with the work presented by Ong et al. (1991a,b, 1992) and Peterson et al. (1994, 1995, 1996), suggest that the greater the soil moisture content, the greater the gas phase concentration of DNT in the soil. Since diffusion in gas is often a more rapid form of transport that diffusion or advection in the liquid phase, a higher gas phase concentration of DNT would lead to a greater flux of the contaminant to and away from the surface, if evaporating conditions are assumed.

2.1. Contaminant Transport Within Soil

Volatile organic solutes, as well as semi-volatile compounds such as 2,4-DNT, display complex behavior in soil as they may be in gaseous, aqueous, and/or sorbed form at any time. To fully describe the transport of volatile contaminant in unsaturated soil, it is necessary to employ a special form of the advection-dispersion equation [2.17].

$$\frac{\partial}{\partial t}(aC_g + \theta C_l + \rho_s C_s) = \frac{\partial}{\partial z}\left(D_g^s \frac{\partial C_g}{\partial z}\right) + \frac{\partial}{\partial z}\left(D_e \frac{\partial C_l}{\partial z}\right) - \frac{\partial}{\partial z}(J_w C_l) - r_s \quad [2.17]$$

Where

D_g^s = *diffusivity of a gas in the porous medium*

D_e = *hydrodynamic dispersion coefficient*

J_w = *water flux*

r_s = *loss of solute per soil volume per time*

and other terms are as described previously. If D_g^s, D_e, J_w, and r_s are measured, then there are three unknowns in this equation: C_g, C_l, and C_s. These are obtained through the phase partitioning equations described previously.

2.2. Contaminant Flux From Soil Surface

The primary interest of this research was to determine the gaseous flux of 2,4-DNT from the soil surface. The phase partitioning and mass transfer relationships convey how 2,4-DNT may come to exist in the gaseous form at the soil surface, but not its behavior after arrival. To understand the mass transfer purely in the gas phase, it is necessary to develop an understanding of Fick's Law of diffusion and the concept of the boundary layer.

2.2.1. Fick's Law of Diffusion

Fick developed a law that describes the transport of a volatile organic contaminant in the gas phase through diffusion. This relationship is defined as:

$$J_g = -D_g^a \frac{\partial C_g}{\partial z} \qquad [2.18]$$

Where J_g is the flux of 2,4-DNT from the soil surface and D_g^a is the diffusivity of a gas in free air.

Fick's law would only apply if the space above the soil was stagnant and infinite. However, in this experiment air flowed over the soil surface and the space above the soil was limited. So, it was necessary to develop an understanding of a mass transfer and fluid flow boundary layer.

2.2.2. 2,4-DNT Mass Transfer Boundary Layer

Jury et al. (1984a) described a mass transfer boundary layer for pesticides. In essence, they equated the mass transfer boundary layer of a pesticide to that of evaporating water. However, Jury's boundary layer fails to take into account the fluid flow boundary layer that would exist when wind is blowing over the soil surface.

A more accurate representation of the mass transfer boundary layer would incorporate the fluid flow or momentum of the gas sweeping across the soil surface. This is achieved by using the following formula (Seinfeld and Pandis, 1999):

$$\delta_c = 0.6 * Sc^{-1/3}\delta \qquad [2.19]$$

Where δ_c is the thickness of the mass transfer boundary layer of 2,4-DNT (cm) and 0.6 is an empirical fitting constant. Sc is the Schmidt number where $Sc = \mu_{air}/D_{air\text{-}2,4\text{-}DNT}$ with μ_{air} being the kinematic viscosity of air (0.156 cm^2/s) and $D_{air\text{-}2,4\text{-}DNT}$ is the binary diffusion coefficient of 2,4-DNT in free air at 25 ^oC. The binary diffusion coefficient of 2,4-DNT in free air was estimated to be 0.002 cm^2/s while the binary diffusion coefficient of water in free air was estimated to be 0.268 cm^2/s using the Fuller correlation at 25 ^oC

(Fuller et al., 1966). Finally δ is equal to the thickness, in cm, of the momentum boundary layer for air, water, and 2,4-DNT where:

$$\delta = 5 * \left(\frac{L}{\mathrm{Re}_L} \right)^{1/2} \qquad [2.20]$$

L refers to the longitudinal distance as measured from some arbitrary fixed point, and Re_L is the Reynolds number as calculated using L as a characteristic length. Since L and the characteristic length used in the Reynold's number are the same equation 2.20 reduces to

$$\delta = 5 * \left(\frac{\mu_{air}}{\rho v} \right)^{1/2} \qquad [2.21]$$

where μ_{air} is the viscosity of air, ρ is the density of air, and v is the air velocity. Therefore, the momentum boundary layer, and consequently the mass transfer boundary layer is inversely proportional to the square root of wind velocity.

3. METHODS AND MATERIALS

The goal of the laboratory experiments was to determine if the surface vapor flux of a point source of (2,4-DNT) could be measured from an unsaturated soil column. In order to create experimental conditions that were reproducible by a computer model and reasonably close to a "real" landmine environment, it was necessary to develop a soil column which could provide both control and measurement of soil moisture content, as well as an ability to control and monitor a sweep gas passing over the soil surface. With these requirements in mind, a column was designed that combined features of both Peterson's et al. (1996) and Spencer and Cliath's (1973) columns. From Peterson, the idea of a sweep gas plenum was used to sweep air over the soil surface in order to induce a net upward movement of both water and contaminant within and from the soil column. Spencer and Cliath's design was useful in controlling the soil moisture content with a hanging column of water located beneath a porous ceramic plate. In addition, it was necessary to measure the soil surface flux of 2,4-DNT, which was accomplished with SPME fibers. Furthermore, to fully understand the behavior of 2,4-DNT within the soil column and at the soil surface it was necessary to measure certain soil parameters that affect 2,4-DNT fate and transport.

The method and set-up for these experiments departed from the work of Jury et al. (1983, 1984a,b,c), Peterson et al. (1996), Spencer and Cliath (1973), and Spencer et al. (1988).

The experiments of Jury et al. (1983, 1984a,b,c) included a stagnant layer of air over the soil surface with no control of soil moisture content. The work of Peterson et al. (1996) was similar to that of Jury et al., except simulated wind blew over the soil surface. Spencer and Cliath's (1973) experiments involved a stagnant layer of air above the soil surface, but included an ability to control soil moisture. Spencer et al. (1988) conducted experiments that allowed simulated wind and control of soil moisture. The contaminant source in all of the experiments presented thus far was present in either a pure crystalline or liquid phase mixed homogeneously with the soil at a given depth. The contribution of the set-up used for the experiments to be presented, was that for the first time both wind and moisture conditions could be set and changed to observe their effect on the contaminant soil surface flux from an aqueous point source contaminant. Furthermore, the effect of simulated rainfall on contaminant soil surface flux after periods of drying had not been investigated with the experimental apparatus of the aforementioned researchers. The experimental set-up presented in this section will allow the examination of this boundary condition.

3.1. Soil Parameter Measurements

The soil used in this experiment was collected at a test minefield operated by Sandia National Laboratories located on Kirtland Air Force Base in Albuquerque, NM. The soil was air-dried, sieved to insure that all soil grains were less than 2 mm in diameter, and mixed to obtain homogeneity. Through soil analysis, it was determined that the soil was a silt-loam with low organic carbon, a low electrical conductivity, and a substantial specific surface area (Table 3.1). The total organic carbon analysis was performed using EPA

method SW846-9060. Electrical conductivity (EC) was measured using the saturated paste method (Rhoades, 1986). Particle size analysis was performed by hydrometer (Gee and Bauder, 1986). Surface area of the soil was determined using the ethylene glycol monoethyl ether (EGME) method (Heilman et al. 1965). A water retention curve of this soil (Figure 3.1) was constructed using both the hanging water column and pressure plate (Soil Moisture Corp., Goleta, CA) techniques (Klute, 1986).

Soil Property	Value
Classification	Sandy Loam
Sand	70.4%
Silt	21.2%
Clay	8.3%
Organic Carbon	0.8%
CEC	10.7
EC	0.92 dS/m
Surface Area	23 m^2/g

Table 3.1. Soil Properties

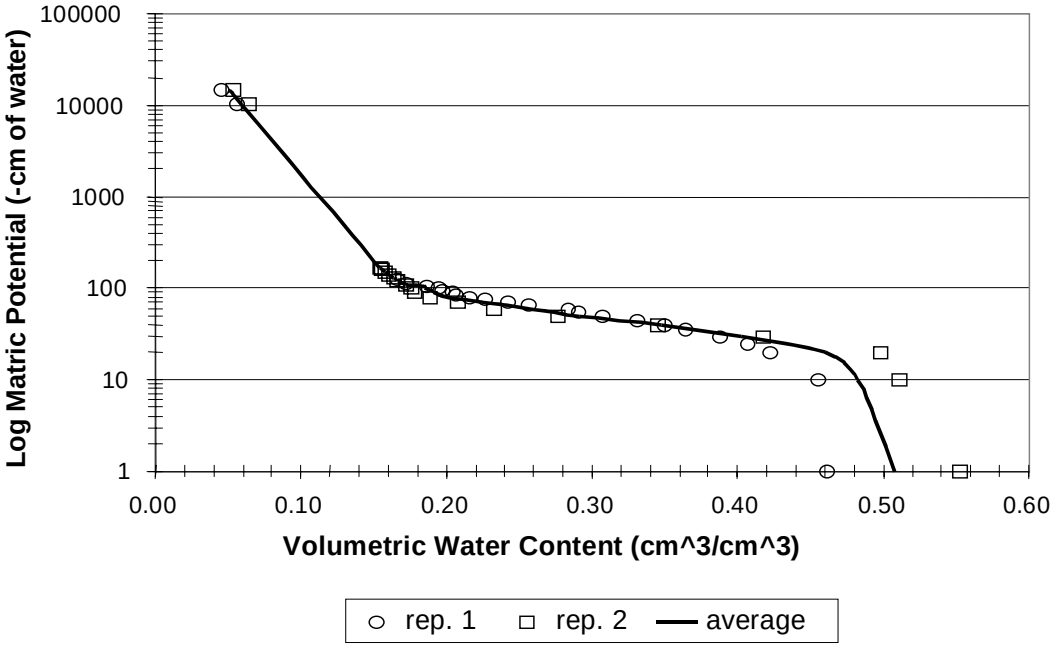

Figure 3.1. Water Retention Curve for Sandia Soil [Solid line represents cubic spline fit of averaged repetitions.]

3.1.1. Aqueous-Solid Distribution Coefficient (K_d,K_f)

Measurements of the 2,4-DNT aqueous-solid distribution coefficient (K_f) were based on the method of Pennington and Patrick (1990) and the Code of Federal Regulations (40 CFR 796) and further explained in a progress report to SERDP (Phelan et al., 1999). Researchers at Sandia National Laboratories measured this distribution coefficient. Aqueous 2,4-DNT solution concentrations of 0.5, 0.75, 1.25, 1.5, 2.0, 25, 50, 75, 100, 125, and 150 mg/L were used to perform this batch test. The sorption behavior of 2,4-DNT on this soil was fitted to a Freundlich isotherm (Figure 3.2) with $C_s = 1.70C_l^{0.82}$ (Fetter, 1999).

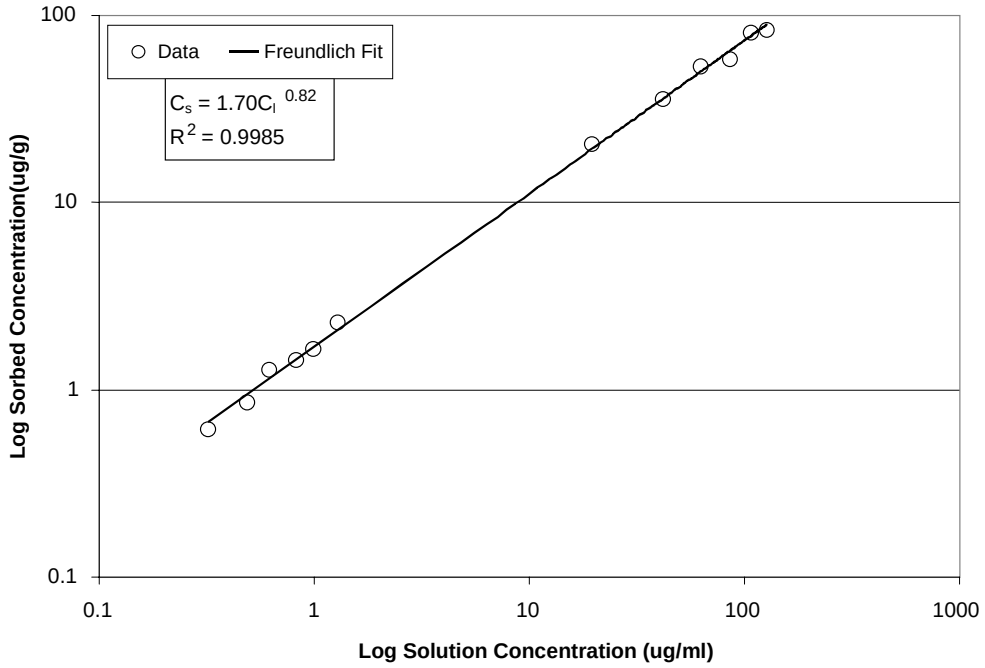

Figure 3.2. Aqueous-Solid Distribution Coefficient (K_f)

3.1.2 K_d' Partitioning Coefficient for 2,4-DNT in Soil Matrix

The aqueous solid distribution coefficient does not give us sufficient information to understand how 2,4-DNT will partition into the gas phase. Henry's law also is

inadequate as sorption of organic contaminants increases with decreasing water content (Ong et al, 1991a,b, 1992, Peterson et al. 1994, 1995, 1996). To fully understand the gas phase concentration of 2,4-DNT within variably saturated soils, the unsaturated soil distribution coefficient (K_d') was also measured at Sandia National Laboratories (Phelan, 1999) (Figure 3.3.). The procedure involved sampling the headspace of a 40-ml volatile organic analyte (VOA) vial that contained soil of various water contents and two concentrations of 2,4-DNT: 6,800 ng/g and 680 ng/g. Headspace sampling was accomplished using 65-µm polydimethylsiloxane-divinylbenzene SPME fibers (Supelco, Bellefonte, PA). The static extraction efficiency of the SPME fibers was determined using the method of Jenkins et al. (1999) and the 2,4-DNT vapor pressure measured by the method of Pella et al. (1977). The data was found to be reasonably well described by the model (Eqns. 2.14-2.16) presented by Peterson et al. (1994, 1995, 1996).

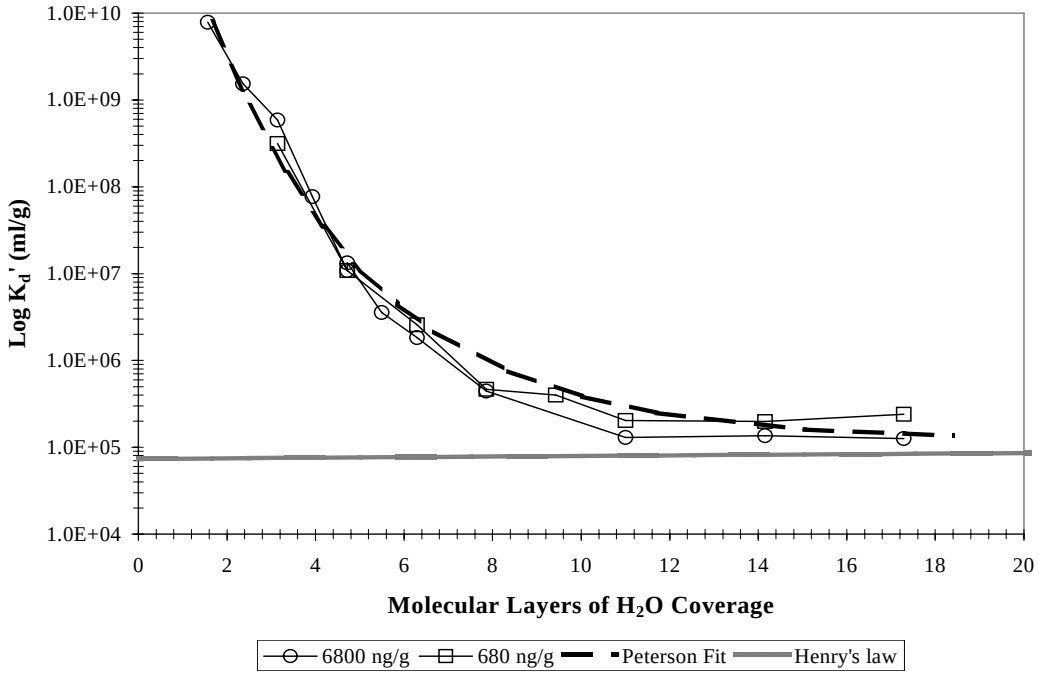

Figure 3.3. K_d' Partitioning Coefficient [Grey line represents the predicted K_d' value (Eqn. 2.13) where Henry's Law should control the gas phase 2,4-DNT concentration]

Using the vapor pressure data (Pella et al., 1977) and water solubility data (Phelan and Barnett, 2000) of 2,4-DNT, the unitless Henry's law constant was estimated to be 9.86E-6 at 23 °C. In attempting to predict the value of K_d' at which Henry's law should control the gas phase concentration of 2,4-DNT (Eqn. 2.13), it was noted that the predicted value did not coincide with the estimated value (Figure 3.3). Peterson et al. (1995) had a similar problem and attributed it to the uncertainty of the K_d value when measured in a batch manner. This appeared to have been the case in this instance as the K_d for 2,4-DNT was measured in a batch manner. Matters were further complicated by having to linearize the K_d sorption isotherm by fitting a straight line through the data points using linear regression. Another possible reason for Eqn. 2.13 not accurately predicting the is that the Henry's law constant for 2,4-DNT has not been experimentally determined.

It further appears (Figure 3.3) that the linear portion of the curve where Henry's law applies to gas phase partitioning ranges from 7.8% volumetric water content, or approximately 10 monomolecular layers of water ($\omega>10$), and greater. However, once the soil moisture content dropped below 7.8% ($\omega<10$) gravimetric the K_d' value increased rapidly. This implied that the lowest sorption, and hence greatest flux, of 2,4-DNT would occur when the soil is in the wet region ($\omega>10$).

These results differed from those of Peterson et al. (1994, 1995, 1996) and Ong et al. (1991a, b, 1992). The soil moisture content where K_d' leveled out and Henry's law began to predict the organic contaminant gas phase concentration is $\omega>10$, rather than $\omega>4$. A

possible explanation for this phenomenon is the relatively more polar nature of 2,4-DNT when compared to TCE. Since 2,4-DNT is more polar than TCE, it would take more water to out-compete 2,4-DNT for sorption sites on the soil surface than it would for TCE.

3.2. Experiment I Set-Up

The experiment was conducted in a 34-cm tall and 14.605-cm i.d. acrylic column (Figure 3.4), which was packed to a dry bulk density of 1.2 g/cm^3. The soil was packed by sprinkling fine lifts of soil (i.e. just enough soil to cover the previous lift) into the column and misting the fine layers of soil with an aqueous 0.005 M $CaCl_2$ solution after each lift. A 1-bar high flow porous ceramic plate (Soil Moisture Inc.) and a water reservoir were fastened to the lower portion of the column. This reservoir was connected by ¼-in tygon tubing to a graduated cylinder, providing a hanging water column to control soil moisture content within the acrylic column.

Along the length of the column, holes were cut to accommodate the insertion of WCR probes and PTFE mininerts. The uppermost mininert, at a depth of 2.9 cm from the soil surface, served as an injection port for a continuous delivery of aqueous phase 2,4-DNT into the center of the packed column from a 5-ml syringe connected to a Cole-Parmer (Vernon Hills, IL) model 74900 syringe pump. A stainless steel plenum (Figure 3.5) was fastened to the upper portion of the column. Essentially, the plenum was two plates separated by 1.25 cm and connected on all sides, with a hole in the bottom. With this design, it was possible to seat the plenum on the column and provide a chamber through

which air could pass over the soil surface. Furthermore, the plenum contained ports through which it was possible to sample the 2,4-DNT surface flux.

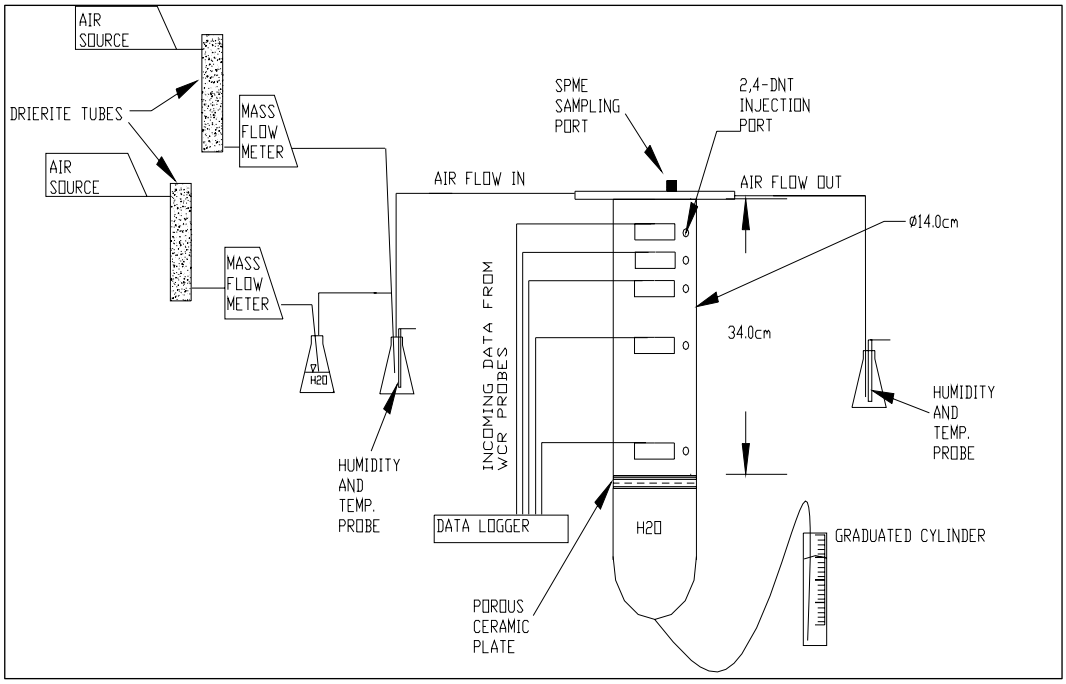

Figure 3.4. Experiment I Set-Up

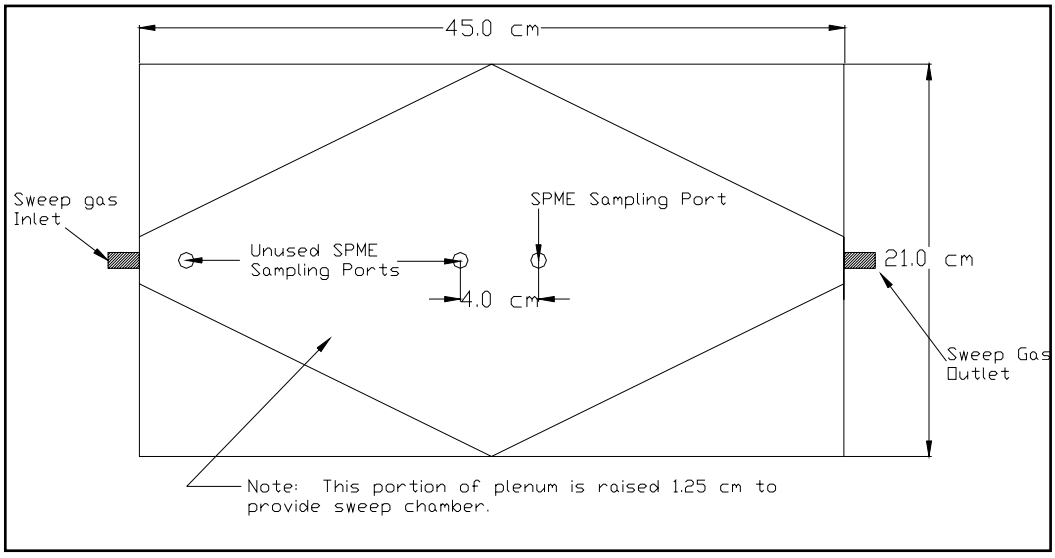

Figure 3.5. Plenum Schematic

3.2.1. Soil Moisture Measurements

Five Campbell Scientific model CS615 water content reflectometers (WCR) were installed horizontally into the column at depths of 2.5, 5.0, 8.9, 15.2, and 31.0 cm from the surface of the column for (Figure 3.4). *(Note: Water content reflectometers are Campbell Scientific's brand name for the more commonly named time domain reflectometry (TDR) probes.)* The rods of each probe had a diameter of 3.2 mm and were cut to a length of 13.2 cm to accommodate the diameter of the column. Each WCR was positioned in a pre-cut hole and sealed with a silicone sealant to prevent water and 2,4-DNT loss. The WCR's were connected to a Campbell Scientific AM-416 multiplexer equipped with a Campbell Scientific model SC32A optically isolated RS232 interface and connected to a Campbell Scientific CR-7 data-logger. Water content was measured every half-hour and collected from the data-logger via a personal computer with Campbell Scientific PC-208 software.

Each WCR probe was installed horizontally and calibrated in a 6-in diameter open-ended PVC cell with a height of 5 cm packed with air-dried soil to a dry bulk density of 1.2 g/cm^3. The top and bottom of each cell were covered with cotton cloth secured with a rubber o-ring. The cells were placed in a flat pan and an aqueous 0.005M $CaCl_2$ solution was added so that each soil cell would imbibe water over-night. The WCRs recorded the reflection time of the electrical wave moving along the WCR rod. This reflection time was compared to the water content determined gravimetrically. Next, each cell was covered with plastic wrap and microwaved with a Daytron model DM4501 microwave oven at a frequency of 2,450 Hz for 3 minutes to drive off and redistribute soil water

(Horton et al, 1982). The cells were then flipped over, so that the bottom of the cell became the top, and again microwaved for 3 minutes. The soil cells were allowed to cool for 2 hours and the cycle was repeated five times. The cycle of five heating and cooling periods followed by WCR electrical wave reflection time and gravimetric water content determination was repeated five times so that a second order polynomial calibration curve could be constructed for each probe.

3.2.2. Surface Flux Measurements

Because the surface flux of 2,4-DNT was expected to be very low and the high degree of sorption of the compound on solid surfaces, sampling the headspace of the plenum with a gas tight syringe was ruled out. Likewise, sampling with a Tenax cartridge was also precluded due to the effective 3×10^6 dilution of contaminant during the extraction procedure. It was determined that the best sampling device to use for the 2,4-DNT was a solid phase micro-extraction fiber. These fibers consist of a small silica fiber coated with a polymer to which contaminants adsorb. Although the surface area of these fibers is small, the benefit of using them is that they effectively concentrate the contaminant, and are easily injected into a gas chromatograph for analysis.

SPME fibers, mounted in a sampling port (Figure 3.5), were used to measure the 2,4-DNT surface flux. These measurements were taken twice daily, except during the first 5 days of the experiment when the 2,4-DNT surface flux did not provide enough mass for analysis.

The dynamic extraction efficiency of the SPME fibers in the plenum was determined experimentally. An oil-less piston pump pulled an air stream from the plenum through an Orbo-79 Tenax cartridge (Supelco). The hole in the bottom of the plenum was sealed with aluminum foil, on which approximately 1 gram of 99% pure crystalline 2,4-DNT (Aldrich, Milwaukee, WI) was placed. The air stream flowed at a rate of ~1 L/min controlled by a metering valve attached to the piston pump and monitored with a mass flow meter (Aalborg). The system was allowed to equilibrate for two days after which a new Tenax cartridge was placed in-line for a period of 30 minutes. During this time, six SPME fibers were sequentially placed in the sampling location for a 30-second duration. This process was repeated three times over the course of three days. Extraction efficiency was calculated as:

$$\%\text{Efficiency} = \frac{\text{(Mass 2,4-2,4-DNT on SPME)/(Minutes of Sampling)}}{\text{(Mass 2,4-2,4-DNT on Tenax)/(Minutes of Sampling)}} * 100 \quad [3.1]$$

The SPME extraction efficiency, as determined by 18 SPME measurements, was determined to be 1.475% of the total 2,4-DNT mass flowing past it with a standard deviation of 0.18%.

Although it was possible to change the height of the SPME fibers in the plenum, it was decided to measure the SPME extraction efficiency with the fibers only positioned approximately 5 mm above the bottom of the plenum. Increasing the depth of the SPME

fibers in the plenum may have provided better extraction efficiency, but it was uncertain what the effects would be if the SPME fiber came in contact with any solid. Since the SPME fibers were always positioned at the same depth in the plenum, the extraction efficiency remained constant and provided an ability to accurately determine the mass of 2,4-DNT emanating from the soil surface.

The SPME fibers and Tenax cartridges were analyzed using a Varian 3400CX gas chromatograph (GC) equipped with a Varian 1078 split/splitless injection port, an electron capture detector (ECD), a 6-m long 530 micron o.d. DB-5 column (J&W Scientific, Folsom, CA), and a personal computer. Furthermore, a Varian 530 μm flash on-column insert (Supelco) for the injection port was utilized to optimize the entry of the analyte into the analytical column.

The GC operating conditions were as described in the proposed EPA method SW846-8095 (USEPA, 1998). This solid waste method was designed by the EPA to analyze common explosive contaminants by GC equipped with an ECD detector. Briefly, the injector is held at 249 °C for two minutes and then ramped to 250 °C at a rate of 10 °C/min. Concurrently the oven temperature program holds the oven at 100 °C for two minutes, then ramps it at a rate of 10 °C/min to a final temperature of 200 °C which is held for zero minutes. The column is then programmed to ramp at a rate of 20 °C/min to a final temperature of 250 °C. The ECD is kept at a constant temperature of 300 °C for the entire duration of the run. The injector, set in the splitless mode of operation,

maintained a flow rate equal to 5 ml/min of He. The column flow rate for He was set to 3 ml/min. The make-up gas was N_2 and flowed through the detector at a rate of 20 ml/min.

The Tenax cartridges were extracted using Occupational Safety and Health Administration (OSHA) method 44 (USOSHA, 1983). Briefly, this method involved separating the large and small portions of the Tenax cartridge and shaking them by hand for 3 minutes in 3 ml of acetone. Each extract was decanted and analyzed for 2,4-DNT. The extract from the smaller portion of Tenax material from the Orbo-79 tube used to determine if breakthrough of 2,4-DNT had occurred

SPME fibers were analyzed by insertion of the fiber into the GC injection port and operating the GC with the aforementioned conditions. This procedure allowed any 2,4-DNT sorbed onto the fiber to desorb, enter the analytical column, and be detected.

3.2.3. Experiment I Conditions

The goal of the first experiment was twofold. First, it was necessary to determine if the 2,4-DNT soil surface flux was substantial enough to measure with SPME fibers. With the first goal realized, it was necessary to keep the top and bottom boundary conditions in the column constant and let the 2,4-DNT surface flux reach steady state. To initiate the experiment, two Badger model 180-22 (Franklin Park, IL) oil-less piston pumps each forced an air stream through drierite traps (Cole-Parmer) to remove water vapor present in the sweep gas air stream. One of the air streams passed through an air-sparging tube into an Erlenmeyer flask filled with deionized water. The dry and humid air streams

were combined to produce a single air-stream flowing at ~1 L/min with ~50% relative humidity (RH). The combined air stream then passed into the plenum and acted as a sweep gas. The RH (%), temperature (^{o}C), and absolute humidity (g/m^{3}) of the air both entering and exiting the plenum were measured with a Vaisala HMP-36B relative humidity sensor and displayed on a Vaisala HMI-36 humidity data processor.

After the column equilibrated with the sweep gas for 2 weeks, a 152.0-mg/L aqueous 2,4-DNT solution was continuously injected at a rate of 1.44 ml/day. Twenty-nine days after injection began, the column experiment was concluded and soil samples collected for both gravimetric water content and 2,4-DNT analysis using a 7/16-inch polycarbonate tube. Nine bore holes were made with five holes equidistantly centered between the WCR rods, and four more holes made perpendicular to the WCR rods and coincident with the air stream axis (Figure 3.6). 1.3 cm depth surface samples were taken at all 9 holes, while samples were taken from the center and four adjacent bore holes every 1.3 cm to a depth of 15.2 cm.

The soil samples were extracted using the EPA SW846-8330 method (USEPA 1994) excluding the salting-out procedure. This procedure involved sonicating approximately 1 gram of soil in 4 ml of acetonitrile in a refrigerated water bath for 18 hours. The supernatant was then decanted, filtered through a 0.45 μm nylon filter and analyzed using a Hewlett Packard 6890 series GC with a thin coat 530-μm o.d 6-meter long RTX-225 column attached to a micro ECD. The GC was further outfitted with a Hewlett Packard

7683 series refrigerated autosampler. Operating conditions were as mentioned for SPME and Tenax analysis.

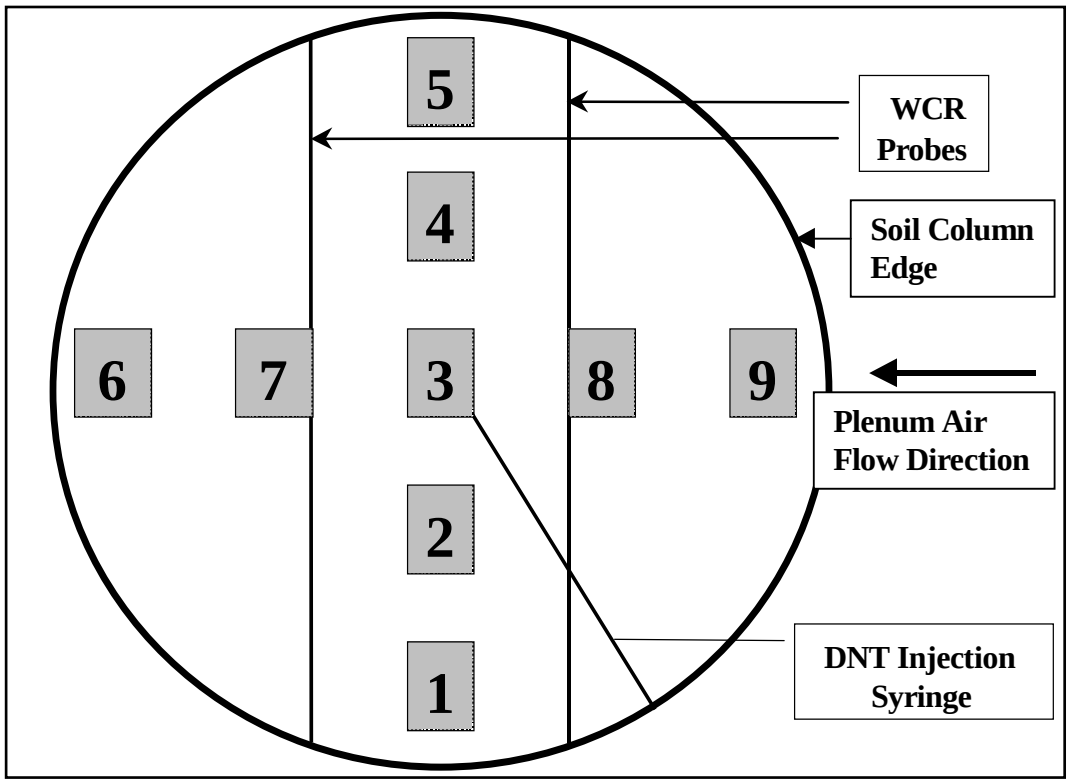

Figure 3.6. Bore Hole Locations

3.3. Experiment II Set-Up

Some changes were made in the experimental set-up for the second experiment. First, sweep gas air was supplied to the plenum via a 20-gallon air compressor, and flow was regulated by two mass flow controllers (Aalborg): one each for the humid and dry air streams. Also the sweep gas entered the plenum 180 degrees from the direction in Experiment I. Before the air from the compressor reached the mass flow controllers it was dehumidified with a drierite trap and any potential contaminants removed by an activated carbon filter. In addition the column and water reservoir were constructed from

schedule-80 polyvinylchloride pipe. Furthermore, the WCRs were now located at depths of 3.5, 6.5, 10.0, 18.0, and 31.0 cm from the soil surface. The aqueous 2,4-DNT was now injected at a depth of 3.6 cm. Other than these set-up modifications, no other changes were made to the experimental design.

3.3.1. Experiment II Conditions

Initially, the second experiment served as a confirmation of the first. The boundary conditions were the same: 50% RH sweep gas air flowed over the soil surface at a flow rate of 1 L/min, matric potential was set at –20 cm below the porous ceramic plate, 1.44 ml/day of a 150.4 mg/L aqueous 2,4-DNT solution was injected into the column, and RH and soil moisture measurements were taken at the same frequency. Furthermore, SPME gas phase measurements were made twice daily, except during the first 10 days when the soil surface flux did not provide enough mass. The aforementioned conditions were Phase I (Steady State) of the experiment. Phase II (Increased Flux) involved setting the sweep gas air to 0% RH and keeping all sampling frequencies the same. Phase III (Drying) was to drop the matric potential to –120 cm below the porous ceramic plate and increase the SPME sampling rate to three times daily. Phase IV (Rainfall I) included taking soil surface samples for gravimetric water content analysis and an addition of 30 ml of water, or an equivalent depth of 0.3 cm, to the top of the column to simulate rainfall. Phase V (Rainfall II) was another rainfall simulation, only this time 63.25 ml of water, or an equivalent depth of 0.6 cm ,was added. During all periods of soil drying and subsequent 2,4-DNT soil surface flux decreases, the stainless steel plenum was replaced with a clean one to determine if desorption of 2,4-DNT off of the plenum was an issue.

The plenum was cleaned by baking it in a temperature-controlled oven at 250 °C for 48 hours. The plenum was then sealed and a SMPE fiber was inserted into the sampling port for a period of 24 hours and analyzed to determine if any 2,4-DNT remained available to partition from the stainless steel surfaces.

4. RESULTS EXPERIMENT I

This experiment was designed to keep the overall volumetric water content of the column at about 25%. From the water retention curve, this would indicate that the matric potential should have been set to about –60 cm of water. It was found that to obtain this moisture content, the matric potential needed to be set to –20 cm of water. The discrepancy was attributed to the repacked nature of the soil. It was also necessary to keep the soil moisture constant during the experiment. Water content during the course of the experiment (Figure 4.1) remained fairly constant with only slight drying (~1% volumetric water content) noted at the top four WCR probes. However, there was an apparent anomaly in the soil water content data as measured at the 2.5 cm depth between days 18 and 21 of Experiment I. This anomaly appeared to have been caused by refilling the injection syringe. The syringe was located just beneath (~4 mm below) the uppermost WCR probe. When the syringe was refilled on day 18, it most likely came in contact with the uppermost WCR probe, decreasing its ability to accurately measure water content. Then when the syringe was refilled on day 21, the syringe most likely lost contact with the WCR probe, returning the measuring properties of the probe to normal.

With soil moisture content and the boundary conditions within the plenum held constant, it was expected that the 2,4-DNT soil emissions (Figure 4.2) would resemble a breakthrough curve for a continuous source contaminant. This was indeed the case as

2,4-DNT sweep gas concentrations rose approximately four orders of magnitude over 26 days.

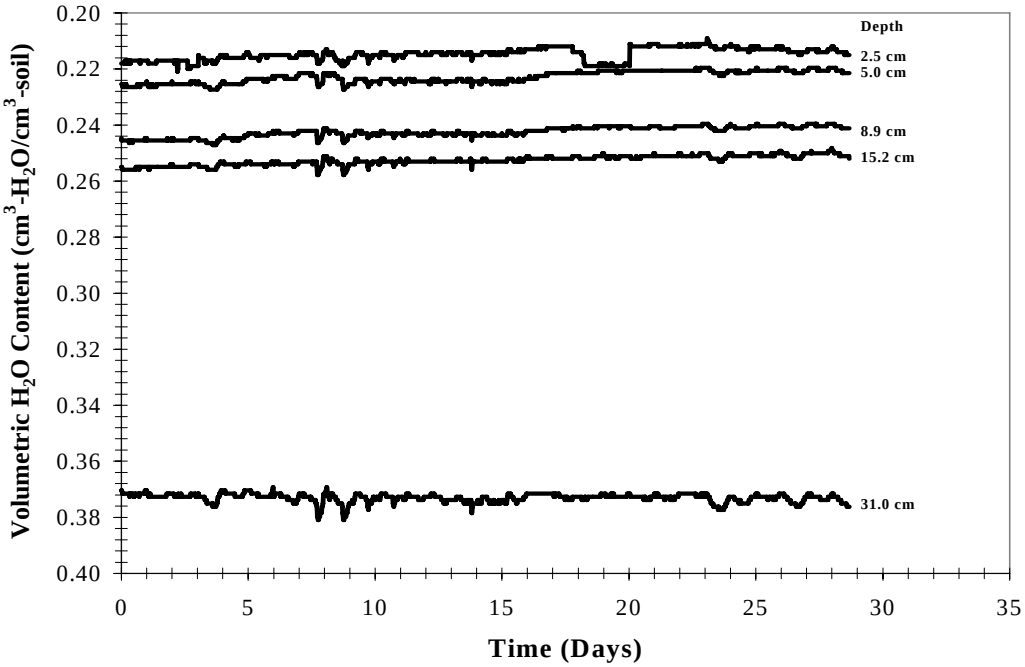

Figure 4.1. Soil Moisture Content Experiment I

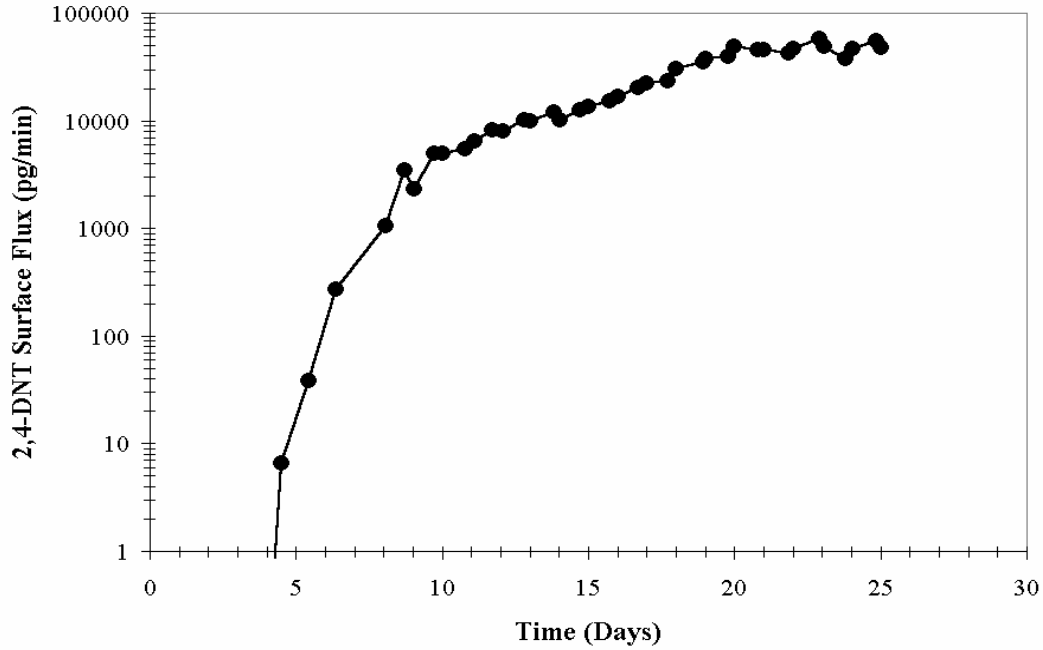

Figure 4.2. 2,4-DNT Soil Surface Flux Experiment I

4.1. Water Mass Recovery Error Analysis

At the end of Experiment I, soil core samples were taken from the column and analyzed for gravimetric water content. This data was compared to the measurements from the last WCR measurement made, and the results were in general agreement (Figure 4.3). For bore holes 2,7, and 8 the WCR soil moisture content falls near the center of bore hole data. However, bore holes 3 and 4 appear to have lower water content than any of the other bore holes or the WCR measurements would indicate. This is attributed to experimental error and the difficulties of taking thin diameter discreet bore hole samples in a small soil column.

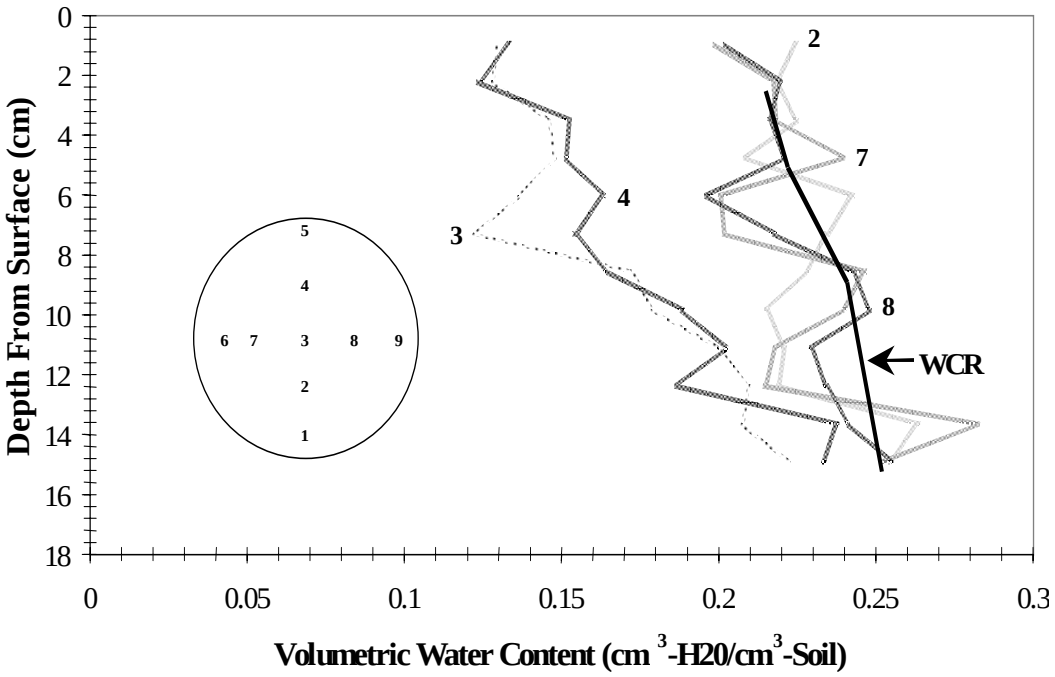

Figure 4.3. Bore Hole Volumetric Water Content vs. WCR Water Content on Day 29 Experiment I

However, the WCR probe is really an average of the water content between the rods of the probe and extending one-inch above and below. Therefore, the bore hole water content data was averaged at each depth increment and compared with the last recorded WCR measurement (Figure 4.4). It can be seen that averaging of the bore hole data smoothes out the data irregularities. Although the source of the relatively lower water contents in bore holes 3 and 4 could not be determined, the WCR measurements more closely correlate with the gravimetric water content data if the data collected from bore holes 3 and 4 are neglected (Figure 4.4). It also appears that the WCR probes were properly calibrated as they only overpredicted the volumetric water content by at most 3% (v/v).

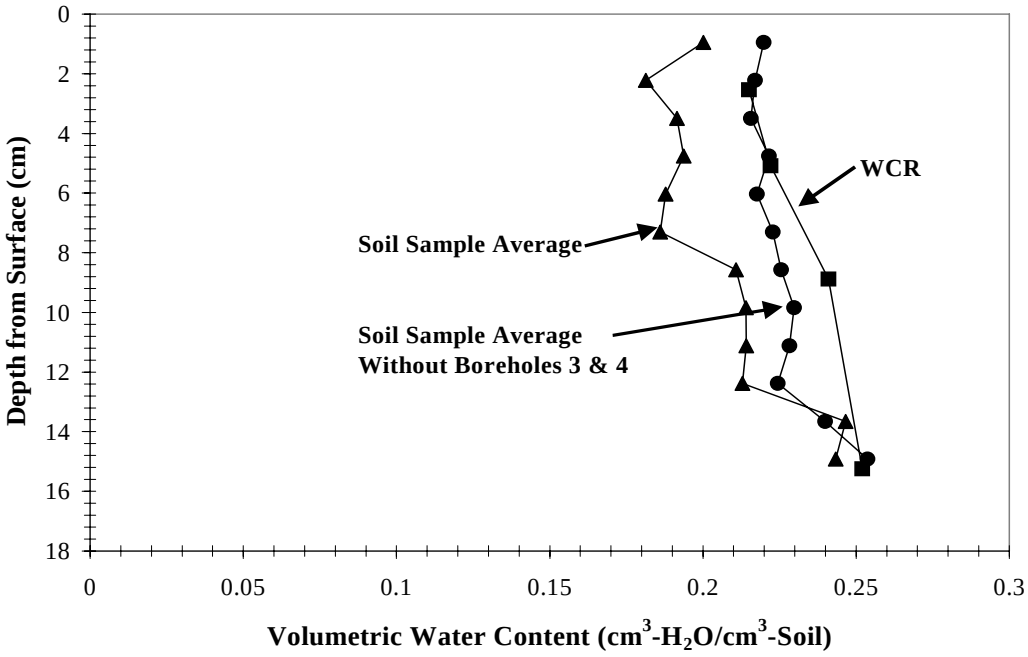

Figure 4.4. Average Soil Volumetric Water Content vs. WCR Water Content on Day 29 Experiment I

4.1.1. Water Mass Recovery Calculations

To accurately depict the water mass recovery, measurement error must be known. The relative humidity probes were a source of error for the water mass recovery. Each probe was calibrated according to manufacturer's specifications. With that accomplished, the manufacturer guaranteed accuracy to within +/- 3% RH. In a related matter, the sweep gas flow rate was measured several times a day and found to be 1.0 L/min with a standard deviation of .05 L/min. A syringe pump with a manufacturer error of +/- 0.001 % controlled the injection of aqueous 2,4-DNT by volume. The syringe pump was calibrated before and after the experiment and found to be 100% accurate to 0.001 ml. Likewise the graduated cylinder used to measure the volume of water passing through the porous ceramic plate was accurate to a volume of 2 ml. Water, probably in the vapor state, was able to escape through tygon tubing, imperfections in the column, imperceptible seal leaks, etc. Before the first experiment began, the soil column was set-up with the exception that the plenum was sealed and no air was passing over the soil surface. The system was allowed to equilibrate with respect to soil moisture content (as evidenced by the WCR probes). Over the course of three days it was noticed that the column lost approximately 1.2 ml water per day, as measured in losses from the graduated cylinder, through imperceptible cracks in the system as well as diffusion though tygon tubing.

In a mass recovery calculation there are three terms to consider: sources, sinks, and changes in storage. The sources in this experiment included water passing through the porous ceramic plate (daily extraction of water from graduated cylinder) and the injection

of aqueous 2,4-DNT into the column (1.44 ml/day). Sinks included evaporation from the soil surface (measured by the RH probes) and the water losses caused by imperfect seals (1.2 ml/day). The only source of storage in this experiment was the soil matrix itself. The change in storage was measured through the WCR probes. This assumes that the volume of soil measured by a WCR probe was equal to the volume enclosed between two planes that intersected the column midway between any adjacent probe or boundary. Therefore, the water recovery was calculated as follows:

$$\text{Water Recovery}\,(\%) = \left(\frac{\text{Evaporation} - \Delta\,\text{Storage}}{\text{Cylinder Water Uptake}}\right) * 100 \qquad [4.1]$$

This water recovery was calculated for every 24-hour increment of time for the duration of the experiment. The average of the daily water recovery was 71% with a standard deviation of 31.7%.

This standard deviation in the water recovery, as calculated with Eqn. 4.1, is high and the source of this appeared to be the change in storage as measured by the WCR probes. For example the average uptake through the column was 15 ml/day with a standard deviation of 2.8 ml/day, while the average evaporation of the column was 11.6 ml/day with a standard deviation of 1.4 ml/day. The imperfect seal water loss and aqueous 2,4-DNT addition were assumed constant. However, the average change in storage was + 0.7 ml/day with a standard deviation of 4.9 ml/day.

Although the calibration data (Fig. 4.4) suggests that the WCR soil moisture measurements are indeed accurate, the extent to which they can be used to calculate storage may be limited, and appears to be the major source of error in calculating the true mass recovery of water in this experiment. This can be attributed to the relatively large volume the lower WCR probes were assumed to measure. For example, small changes in the water content at the bottom WCR probe would cause large changes in storage, because it had to be assumed that the lowest WCR probe could measure the water content of a relatively larger section of the column. A solution to this problem would be to have the WCR probes evenly spaced throughout the column at very close intervals. Therefore, at best, we can only estimate a total mass recovery of water for this and the following experiment.

4.2. 2,4-DNT Soil Surface Flux

Over the course of 25 days, boundary conditions in the soil column were kept constant and measurements of the surface flux were made. As was anticipated, the surface flux of 2,4-DNT (Figure 4.2) resembled the breakthrough curve for a continuous point source contaminant. Furthermore, the surface flux appeared to be at or near steady state after day 20 of the experiment. Since the goals of the experiment had been achieved (i.e. assessment of experimental set-up and steady state surface flux), the experiment was concluded. Since the impetus for this experiment was to determine if the computer code that was being used to model this data was performing properly, the decision to end the experiment was also made in order to compare the experimental data with the model's predictions.

4.3 2,4-DNT Soil Column Concentrations

Since the computer code developed at Sandia National Laboratories was also capable of predicting concentrations within the soil, it was deemed necessary to take discreet soil samples as a method of evaluating the model's performance. The sampling and subsequent analysis revealed that 2,4-DNT concentrations were greatest closest to the injection point and in the center bore hole (Figure 4.5). It was noted that, potentially due to an undetected irregularity in soil packing, the concentrations of 2,4-DNT in bore hole 7 became non-detect at depths greater than 8 cm. With this information in mind, contaminant flow in this column cannot be viewed as one-dimensional. Three dimensions would be an ideal situation, however it was impossible to characterize all of the imperfections in the soil packing. These imperfections would include any cracks or grain sorting that could contribute to either heterogeneity or anisotropy within the soil column. Without the ability to describe the soil matrix on the pore scale, it was best to view the 2,4-DNT concentrations with depth as a function of two dimensions: r and z in the polar coordinate system.

Averaging the bulk soil 2,4-DNT soil concentrations at each depth increment with respect to radial distance from the center bore hole provides a clearer picture of the 2,4-DNT distribution within the soil column (Figure 4.6). The concentration of 2,4-DNT in the bulk soil is indeed higher in the center bore hole than at a radial distance of 2.5 cm.

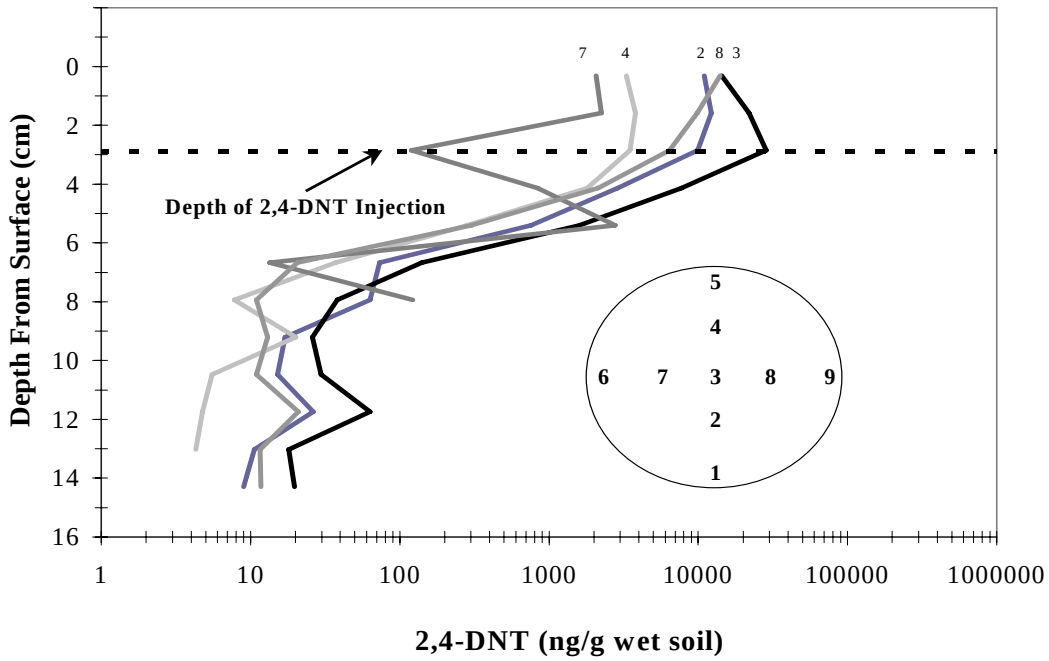

Figure 4.5. Bore Hole 2,4-DNT-Soil Concentrations Experiment I

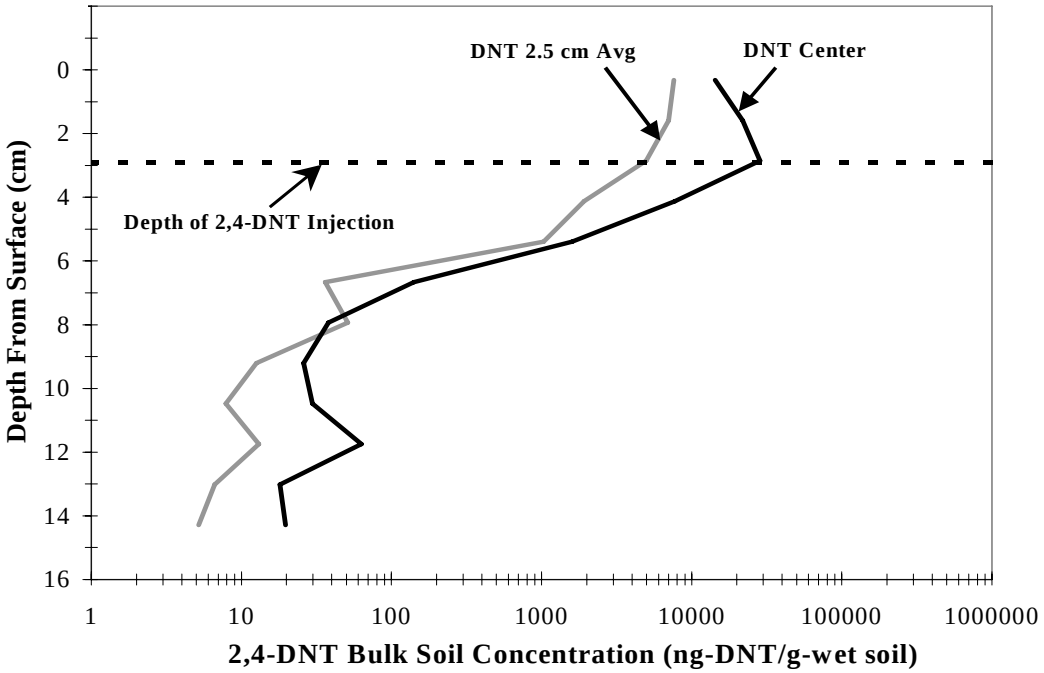

Figure 4.6. Avg. 2,4-DNT-Soil Concentrations at 2.5 cm Radial Distance and Column Center Experiment I

Due to the evaporative flux of water, the dominant movement of both contaminant and water should have been upward. However, the 2,4-DNT appears to also have traveled downward beneath the injection point at approximately 2.9 cm beneath the center of the column. It seems that either cross contamination during soil sampling or gravity drainage may have played a role in the 2,4-DNT transport during the experiment. Cross contamination should have been limited as the surface area of the sampling tube was low compared to the soil surface area. Concerning the gravity drainage theory, the injection of aqueous 2,4-DNT was kept constant at 1.44 ml/day and the average evaporation as measured by the relative humidity probes was 11.55 ml/day with a standard deviation of 1.36 ml/day. Thus, the injection of 2,4-DNT was approximately 12.5% of the evaporation. Moreover, the aqueous 2,4-DNT was injected at a single point and evaporation occurred over the entire soil surface. All of these factors combined, would suggest that at the 2,4-DNT injection point, there was some localized gravity drainage, but overall evaporation and upward movement was the dominant mode of transport for both water and 2,4-DNT.

4.4 2,4-DNT Mass Recovery

An attempt to determine a mass recovery for 2,4-DNT within the experimental set-up was made. However, this mass recovery can only be viewed as an estimate. The only variable that was known absolutely was the mass of 2,4-DNT put into the system (6,400,000 ng-2,4-DNT). The mass emitted from the soil surface was calculated by finding the area under the curve in Figure 4.2. The total 2,4-DNT soil concentration can

only be estimated, because the entire soil mass within the column was not extracted and analyzed; only discrete soil samples were taken for reasons previously mentioned. The last portion of the mass recovery has to include the amount of 2,4-DNT that sorbed onto surfaces in the column and plenum. These measurements could not and were not made due to the inability to extract 2,4-DNT from either of these complex geometric surfaces.

4.4.1 Total Surface Flux Calculations

Estimating the entire amount of 2,4-DNT emitted from the soil surface was done by integrating the area under the surface flux curve (Figure 4.2) using the trapezoidal rule. The height of each side was the value of surface flux for two adjacent flux measurements, while the width was equal to the increment of time between the same two adjacent flux measurements. The area between any two points can then be calculated as

$$A = \frac{1}{2} h(a + b) \qquad [4.2]$$

where A is the area under the portion of the surface flux curve under consideration (also the total surface flux for the same time period), h is the time interval, while a and b are the two surface flux measurements.

Once this calculation was performed on every pair of adjacent surface flux measurements (Figure 4.2), the total mass emitted from the soil surface during the course of the experiment was found to be 610,000 ng-2,4-DNT.

4.4.2 Total 2,4-DNT Soil Calculations

Since the entire mass of soil was not analyzed, the total mass of 2,4-DNT in the soil was estimated from discreet soil samples. A mass per volume approach was taken using two geometries to describe the entire volume of soil to a depth of 15.24 cm; the 2,4-DNT-soil concentrations were not measured below this point, and estimating their concentrations would have been conjecture.

The first geometry is that of a cylinder with a 7/16-in diameter and a depth of 15.24 cm. This geometry describes the center bore hole (bore hole 3). This volume contained 12 cylinder volumes each with the same diameter and a length of 1.27-cm to represent each of the discreet soil samples taken. Since the samples were analyzed to obtain the mass of 2,4-DNT per wet weight of soil, the concentrations had to be converted to mass per volume of soil. This was accomplished by estimating the wet bulk density of the soil by adding the dry bulk density (1.23 g-soil/cm^3-soil) to the average of all gravimetric water contents at each depth increment. Then the mass of 2,4-DNT per volume was calculated by multiplying the mass-2,4-DNT/ mass-wet soil by the estimated wet bulk soil density. Finally to obtain the mass for the entire first geometry was a matter of summing the mass for each of the 12 individual elements and was equal to 130,000 ng-2,4-DNT.

The second geometry was again a cylinder with a depth of 15.24 cm, but the diameter was now 14.75 cm, or the entire diameter of the column minus the diameter of the first geometry. The second geometry was divided up into 12 elements according to the discreet samples taken every 1.27 cm. The mass of 2,4-DNT per unit volume was

calculated by averaging the 2,4-DNT concentrations for each 1.27 cm depth interval in bore holes 2,4,7, and 8. This averaged concentration was assumed to be representative of the 2,4-DNT concentration for the entire element corresponding to each depth element. Finally the sum of the mass of 2,4-DNT within each of the 12 elements was totaled. The mass for the entire second geometry was 7,000,000 ng-2,4-DNT.

4.4.3. 2,4-DNT Mass Recovery Summary

The total mass injected into the column during the course of experiment was 6,400,000 ng-2,4-DNT. Using the estimations previously described the mass of 2,4-DNT residing in the soil column was 7,130,000 ng-2,4-DNT, and the amount of 2,4-DNT that was emitted from the soil surface was 610,000 ng. Therefore calculating mass recovery as

$$\text{Mass Recovery}\,(\%) = \frac{\text{Mass DNT(Soil)} + \text{Mass DNT(Emitted)}}{\text{Mass DNT Injected}} * 100 \qquad [4.3]$$

the percentage of 2,4-DNT measured is 121% of that injected, or 21% more than was injected into the column.

Most of the error associated with this calculation was from not analyzing the entire soil column for 2,4-DNT. The estimation of 2,4-DNT in the column is an overestimate, because it was assumed that the average of the 2,4-DNT-soil concentrations at the first radius of bore holes was representative of the concentration for the entire radius of the column. In reality, however, concentration decreased radially from the center of the column. Further error was introduced by not being able to analyze the surface of both the

column and plenum for any residual 2,4-DNT. However the error stemming from this should be small as the surface area of the top 15.24 cm of the column and entire plenum is only equal to 1,997 cm^2, while the surface area of the soil in the top 15.24 cm of the column is $5.83*10^9$ cm^2. Sorption of 2,4-DNT to the soil phase is much more important than sorption to either the column or the plenum.

4.5 Data Model Comparison Experiment I

Since the impetus for conducting these experiments was to calibrate a computer model, it is of some interest to observe how the model performed. The code used for modeling laboratory results was T2TNT, a modification of the TOUGH2 family of codes (Webb et al., 1999). The modifications were made so that the code could evaluate the conditions related to the landmine problem.

The input parameters for the model were as follows: 1) the water retention curve (Figure 3.1), 2) the K_d' sorption isotherm (Figure 3.3), 3) a dry bulk soil density of 1.2 g/cm^3 4) Henry's law constant, 5) a mass transfer to momentum boundary layer ratio of 0.5, and 6) a linearized aqueous-solid sorption isotherm with $C_s=0.7C_s$. The first four parameters were as measured and described in sections 3. through 3.2. However, there were some uncertainties in the last two parameters used for model calibration. The first uncertainty was with the mass transfer boundary layer ratio of 2,4-DNT to the water vapor.

Using the relationships presented in section 2.2.2., the thickness of the mass transfer boundary layer above the soil surface can be calculated. It is important to remember that

the mass transfer boundary layer will only exist over the soil surface where mass transfer occurs, while the momentum boundary layer will exist everywhere gas flow is present. Both the momentum and mass transfer boundary layers have been calculated and plotted in Figure 4.7. The heights of the momentum and water mass transfer boundary layers exceed the top of the plenum. As a result, there will never be a point at which the water concentration in the sweep chamber air will be zero as long as there is evaporation. This has two important implications: 1) The model of Jury et al. (1983, 1984a, b, c) cannot be used here as it assumes that at some distance above the soil surface the gas phase concentration of both contaminant and water will be zero; and 2) a diffusion-driven gas phase water vapor concentration gradient will exist, but it will never approach zero in the plenum.

Other methods of predicting the size of the boundary layers calculated different values for the mass transfer to momentum boundary layer ratio. It was decided by researchers at Sandia National Laboratories (Phelan et al., 2000) to set the boundary layer ratio to a value of 0.5 as it was impossible to experimentally determine the ratio and it allowed the model to provide a better fit to the experimental data.

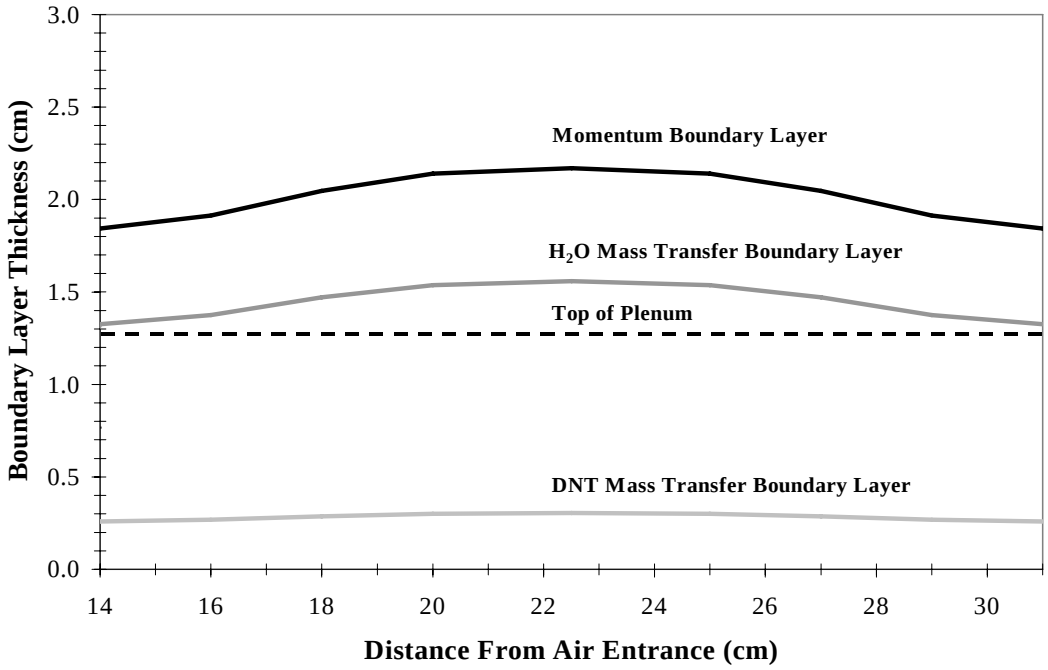

Figure 4.7. Momentum and Mass Transfer Boundary Layers for H_2O and 2,4-DNT

The last and perhaps most significant uncertainty was in the value of the aqueous-solid partitioning coefficient (K_d). As mentioned earlier the K_d value was measured during batch equilibrium tests. When the K_d is determined in such a manner, the 2,4-DNT may have a chance to react with all sites on the soil particle due to the high water to soil ratio. In this experiment, the soil was unsaturated and the 2,4-DNT could not react with every site due to the contact of adjacent soil particles. Therefore, the measured K_d is probably high. Furthermore, T2TNT was not yet capable of handling Freundlich sorption so the isotherm had to be linearized by computing the best-fit line through the data using linear regression analysis.

With these parameter uncertainties in mind, the experiment soil-data and model predictions were compared and found to be favorable (Figure 4.8). Output from the model was selected at depths of 0 to 15 cm below the soil surface. Since T2TNT is a two

dimensional model, outputs at 0 and 2.9 cm from the center of the column were appropriate. As was anticipated the center bore hole and the model prediction for that location produced the highest soil concentration of 2,4-DNT. However, the model seems to have predicted some localized gravity drainage as the peak 2,4-DNT concentration from the center of the column appears to be approximately 1 cm lower than the depth of injection (Figure 4.8). At the 2.9 cm radial distance, the model predicted 2,4-DNT concentrations that fell approximately in the center of all data obtained at that radial distance. This was another indication the model was performing well.

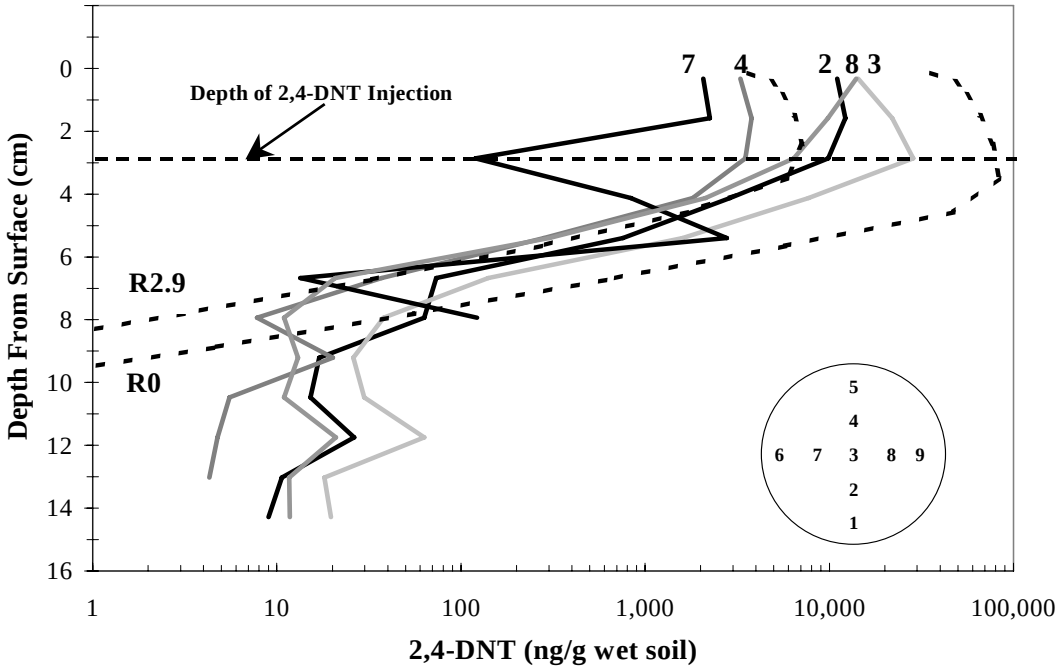

Figure 4.8. Soil Data-Model Comparison Experiment I of 2,4-DNT Concentrations vs. Depth. Dashed Lines are Model Simulations

The experimental flux data and model predictions were compared and found to be favorable (Figure 4.9). However, the model seems to have overpredicted the initial 2,4-DNT surface flux. This may be due to the low concentrations of 2,4-DNT measured for the first few data points, resulting in data that may have been biased low.

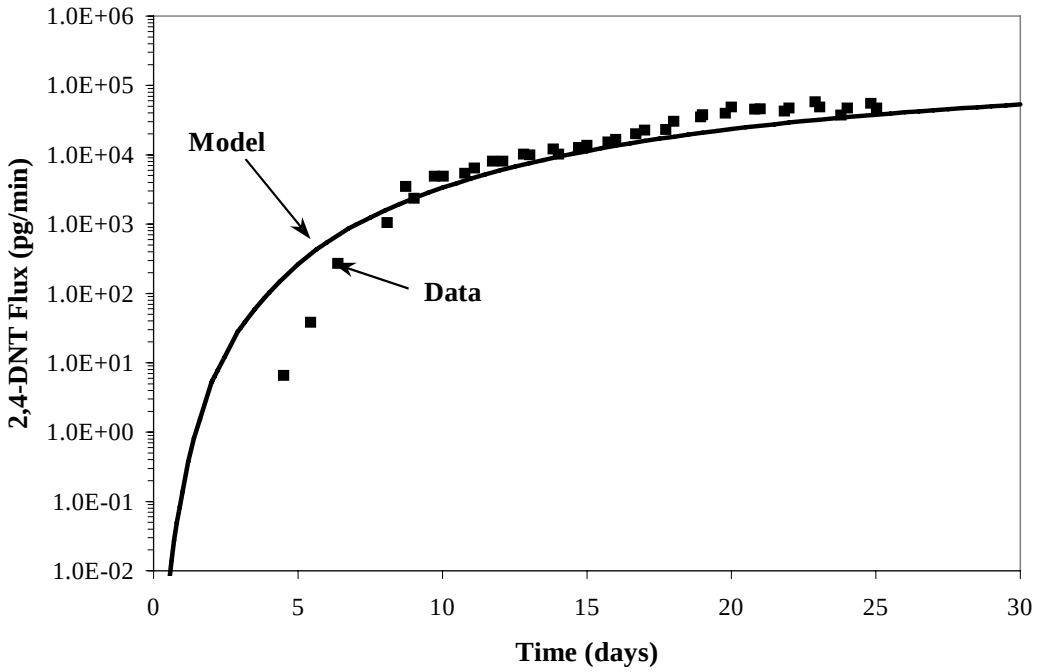

Figure 4.9. Data Model Comparison-Experiment I

With the problems of detecting very low concentration fluxes and the uncertainties of the K_d sorption isotherm and the mass transfer to momentum boundary layer ratio present, T2TNT was still able to adequately predict the experimental results. In the future, a column test will be performed to determine the value of the aqueous-solid distribution coefficient from the shape and timing of the 2,4-DNT break through curve. In addition, T2TNT was modified to handle non-linear sorption for all future experiments.

5. RESULTS EXPERIMENT II: VARYING BOUNDARY CONDITIONS

The goal of Experiment II was to change the boundary conditions at the top and bottom of the soil column to evaluate changes in 2,4-DNT flux. Specifically, it was of interest to determine how the 2,4-DNT surface flux would perform under equilibrium conditions similar to Experiment I, drying, and wetting. Therefore Experiment II was broken up into several phases. The 2,4-DNT surface flux in the Experiment II was more dynamic than in Experiment I due to the variation of both the top and bottom boundary conditions during the course of the experiment (Figure 5.1). The soil moisture content in the column followed suit and varied considerably (Figure 5.2) as a result of changing boundary conditions.

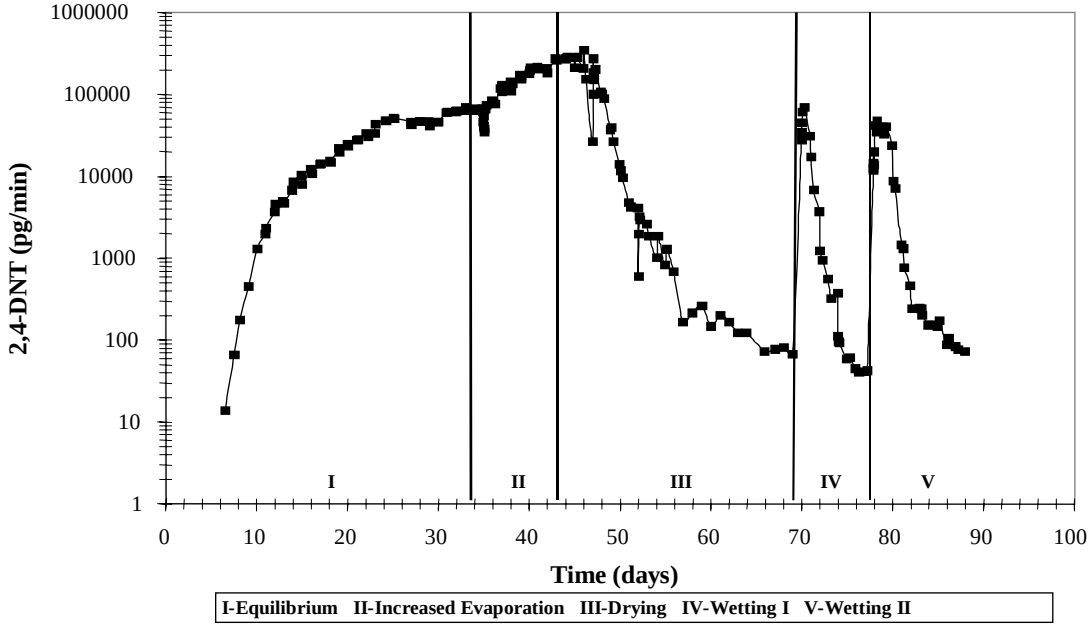

Figure 5.1. 2,4-DNT Soil Surface Flux-Experiment II

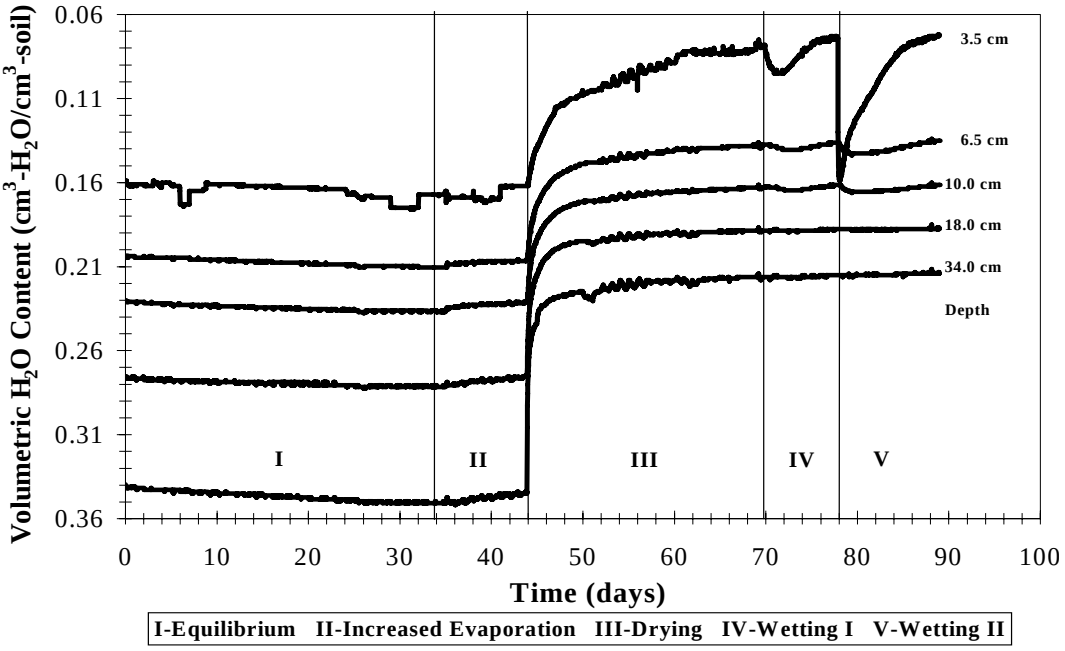

Figure 5.2. WCR Volumetric Water Content-Experiment II

5.1. Water Mass Recovery Error Analysis

At the end of Experiment II, discreet soil samples were taken in the same manner as those for Experiment I (Figure 3.6). Again the soil moisture samples for each bore hole and the averages of the soil moisture contents at each depth increment were compared with the WCR soil moisture measurements (Figure 5.3 and 5.4).

It appears that for Experiment II some of the difficulties of taking discreet soil samples in the column were overcome. The water content profiles at the depths for each bore hole (Figure 5.3) are all closely related to the WCR water content. In fact, the volumetric water content as measured by the WCRs had absolute errors of 1.49%, 2.40%, 0.79%, 2.45%, and 1.98%, when compared to the averaged gravimetric water content measurements of the soil samples in bore holes 2,3,4,7,and 8.

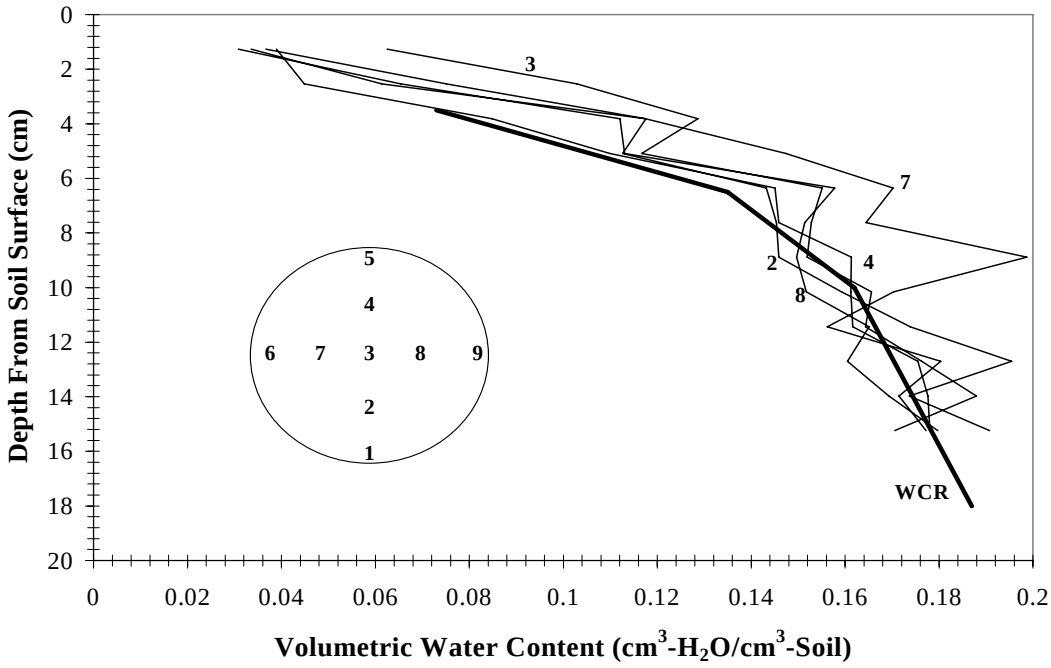

Figure 5.3. Bore Hole Volumetric Water Content vs. WCR Water Content on Day 89 Experiment II

The average water content as a function of depth was also compared with the last WCR measurement made (Figure 5.4) and results were again favorable. The average absolute error for this comparison was 1.66% volumetric water content. However, the WCR's seemed to underestimate the water content in this experiment, while for Experiment I they overestimated water content. This was due to the water content at the end of experiment being significantly drier than that of Experiment I. When the WCR probes were calibrated, the soil within the calibration cell would crack when volumetric water contents got much below 10%. Therefore, there is less confidence when the WCR's are used to measure water content for dry soils. This can be observed in Figure 5.4 where the soil samples and the WCR measurements seem to converge at volumetric water contents greater than 15% volumetric.

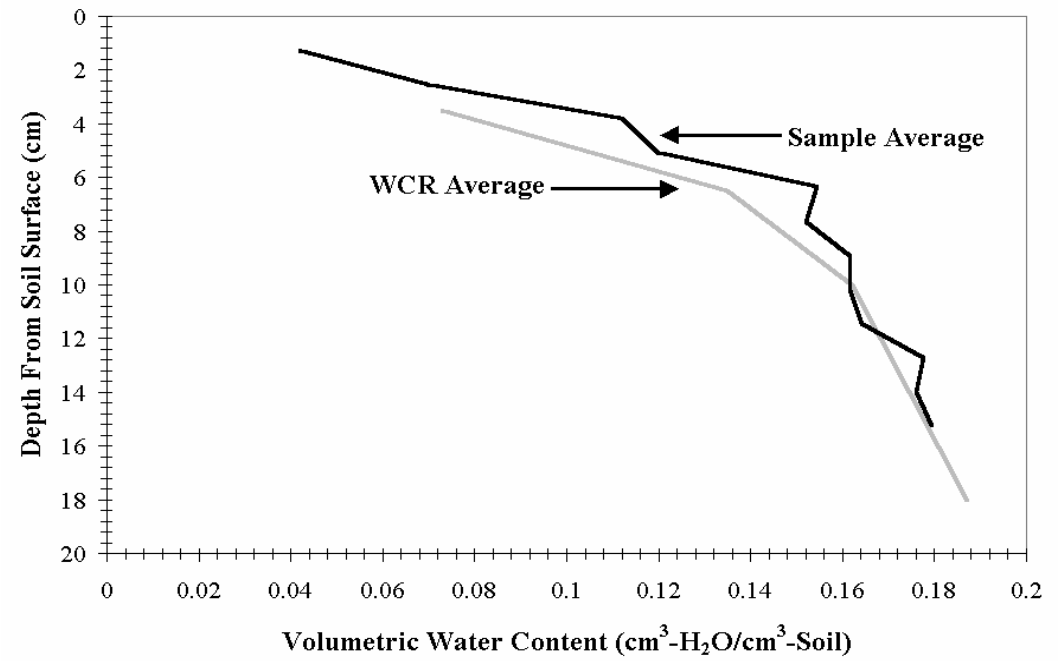

Figure 5.4. Average Volumetric Water Content vs. WCR Water Content on Day 89 Experiment II

5.1.1. Water Mass Recovery

All calculations and errors associated with the water mass recovery calculations for Experiment II were identical to those performed for Experiment I, and as described in sections 4.1 through 4.1.1. Using Equation [4.1], it was found that the average daily water mass recovery was 83.1% with a sample standard deviation of 79.4%. The standard deviation is very large, and again this is due to the same problem that plagued the water mass recovery for Experiment I: storage as measured by the WCRs. Experiment I had constant boundary conditions, in Experiment II, however, there were several changes in boundary conditions which caused drying and wetting of the soil. Since the WCRs were not more closely spaced it is difficult to determine the true storage of water, especially since water content throughout the column changed several times. In

fact, the variable boundary conditions appear to have exacerbated the problem caused by the storage term.

5.2. 2,4-DNT Surface Flux Phase I (Equilibrium)

During Phase I (Equilibrium) the surface flux nearly replicated that of the Experiment I. When the two data sets were compared, 2,4-DNT flux measurement to flux measurement on corresponding days up to day 25, the correlation coefficient was 0.953 and the F-test proved to be equally good with a result of 0.52 at the 0.05 level of significance. The 2,4-DNT flux for Experiment II was slightly lower than that of Experiment I for any corresponding day. This might be attributed to the drier soil conditions of Experiment II (Figure 5.2 vs. Figure 4.1). However, the statistical tests above eliminate the possibility of a significant difference between the two data sets.

The volumetric water content, as evidenced by the uppermost WCR probe, remained essentially constant at approximately 16% (Figure 5.2) during Experiment I. So the flux curve (Figure 5.1) should behave as a breakthrough curve for a continuous point source contaminant. This was indeed the case. Furthermore, the water content was greater than 7.8% volumetric. According to the discussion in Section 3.1.2, this would indicate that enough water was present in the bulk soil to out-compete 2,4-DNT for sorption sites on the soil surface and allow for Henry's Law to be the applicable partitioning relationship for 2,4-DNT in this phase of Experiment II.

5.2.1 Phase II (Increased Evaporation)

Phase II (Increased Evaporation) was initially designed to dry out the soil surface to facilitate a decline in 2,4-DNT surface flux. However, due the apparent high hydraulic conductivity of the soil as packed, water was able to pass through the porous ceramic plate at the lower boundary of the column and be supplied to the surface very quickly. As a result, the soil did not dry out significantly (Figure 5.2), but evaporation did increase from an average of 8.36 to 23.50 ml/day. This was simply a result of liquid phase water flowing from high concentration in the soil to a relatively lower concentration (RH decreased from 50% to 0%).

Furthermore, the soil volumetric water content decreased slightly at the uppermost WCR probe (Figure 5.2). However, in Phase II, as in Phase I, the soil moisture content did not drop below 7.8%. So, as discussed in section 3.1.2., the soil was still in the moisture regime where Henry's Law would be the applicable partitioning coefficient for 2,4-DNT. However, the 2,4-DNT flux increased by an order of magnitude during this 10-day phase. This flux increase was not connected with increases in soil moisture content, but with the increased water flux rate. As the evaporation rate increased, the contaminant could move more quickly to the soil surface in the water phase. After reaching the soil surface, the greater mass of 2,4-DNT was then available to volatilize.

5.2.2 Phase III (Drying)

After letting Phase II run for ten days the soil column was dried out by increasing the matric potential at the porous plate another meter: from –20 to –120 cm-H_2O of matric

potential. This was Phase III (Drying) of the experiment. Increasing the matric potential had the obvious effect of drying the soil within the column, but it also caused some downward movement of water as the column drained. In fact, as the water drained from the column, the water content at the uppermost WCR probe indicated that the volumetric moisture content near the surface dropped from 15.5% to 8.2%. As discussed in Section 3.1.2., soil moisture content is critical in determining how much 2,4-DNT will be in the gas phase. In order to have a calibration point for the model developed at Sandia National Laboratories, and to have concrete evidence of the soil moisture conditions at the soil surface, it was decided to take four samples form the soil surface from locations 2,4,7, and 8 in Figure 3.6. to a depth of approximately 0.5 cm at the end of Phase III. This data (Table 5.1.) suggests that the soil moisture content was in the drier range where the amount of 2,4-DNT in the gas phase would be diminished and the amount sorbed onto the soil would be increased. As discussed in section 3.1.2., this provides the appropriate conditions for the surface flux of 2,4-DNT to decrease. This was evident during Phase III of Experiment II, as the 2,4-DNT flux decreased almost 4 orders of magnitude during this 24-day period.

Bore Hole	Volumetric Water Content (%)
2	3.81
4	4.11
7	4.05
8	3.62

Table 5.1 Bore Hole Locations and Volumetric Water Contents at Phase III/IV Boundary

Desorption of 2,4-DNT off of the plenum was a concern during this phase of the experiment. To eliminate any possibility that desorption of 2,4-DNT from the plenum

was masking the true decline in 2,4-DNT soil flux, the plenum was changed on day 47 and day 52). The first time the plenum was replaced a small crack was noticed on the soil surface, presumably due to drying and mechanical vibration of the column during plenum removal. This complicated matters as it was not clear when the crack had actually developed. Furthermore, the 2,4-DNT flux was no longer coming exclusively from the soil surface, but also from the fast path developed by the soil crack. Therefore the 2,4-DNT flux during this and all subsequent phases of the experiment may have been artificially high due to the presence of the soil crack at the surface.

The second plenum change at day 52 showed that the kinetics of 2,4-DNT desorbing from the plenum were not significant. When the plenum was changed there was an initial apparent decrease in soil surface flux due to the availability of fresh sites for 2,4-DNT sorption. This lasted approximately 12 hours. However, once the new plenum came into equilibrium with the 2,4-DNT surface flux, the data seemed to follow the same trend as before. Therefore, the true surface flux was not being masked by desorption of 2,4-DNT from the surface of the plenum.

5.2.3. Phase IV (Rainfall I)

Phase IV (Rainfall I) was designed to determine what effect rainfall would have on 2,4-DNT flux after a period of drying. After the soil moisture content samples were taken at the Phase III/Phase IV boundary and rainfall simulated, the surface flux increased approximately three orders of magnitude during the subsequent 8-hour period. After simulating rain, it was visually noted that the soil surface appeared saturated, and some

ponding of water occurred. This indicated that although the uppermost WCR probe only registered an increase in volumetric water content from approximately 8.0% to 9.2%, the water content at the soil surface was greater and probably and probably much greater than indicated by the upper-most WCR probe. As discussed in Section 3.1.2., when soil volumetric moisture content is greater than approximately 7.8%, water will out-compete 2,4-DNT for soil sorption sites. Therefore, 2,4-DNT will be largely partitioned, in the gas phase and available to emanate from the soil surface.

Again, as the soil was wetted, the water preferentially sorbed onto the soil surface, freeing most of the soil sequestered 2,4-DNT to volatilize and caused a three order of magnitude increase in 2,4-DNT flux . However, this peak in 2,4-DNT flux may have been exacerbated due to the soil samples collected at the Phase III/Phase IV boundary. As some of the soil surface was removed, the 2,4-DNT laden soil that was previously beneath the surface was exposed, allowing for a potentially higher surface flux. It was due to this and the fact that the top WCR probe only registered an approximate 1.2% increase in volumetric water content (Figure 5.2), that a second wetting phase was performed.

Although the 2,4-DNT surface flux declined more quickly after the soil surface had dried than in Phase III, it appeared that, again, sorption of 2,4-DNT from the plenum was not significant. On day 74 of the experiment, the plenum was changed for a third time. The trend of surface flux decline was unaffected except for an initial decrease in 2,4-DNT flux for reasons previously discussed.

5.2.4. Phase V (Rainfall II)

After the soil moisture content, as measured by the top WCR probe, returned to its previous value (approximately 8% volumetric water content), Phase V (Second Wetting) commenced on day 78. The goal of the second wetting event was to increase the soil moisture content measured by the top WCR to 15% volumetric. The addition of water to simulate rainfall had the intended effect, and within 30 minutes brought the volumetric water content at the top probe up to 16.5% from 7.9%. The experiment was concluded when the moisture content at the upper most WCR probe reached a value near the moisture conditions prior to the second rainfall simulation.

As in Phase IV, the 2,4-DNT surface flux rapidly increased almost four orders of magnitude within a few hours after the simulated rainfall. The highest flux value after this rainfall was ~47,000 pg/min while after the first rainfall the highest recorded flux was ~70,000 pg/min. This discrepancy can be attributed to two factors. The first factor is that prior to Phase V, no soil surface samples were collected. Thus no buried soil was freshly exposed and no 2,4-DNT could be sorbed off of it. Secondly, the amount of water added to the soil surface was nearly doubled. Therefore, more of the 2,4-DNT could have been dissolved and transported in the downward moving water.

Although the initial increase in flux was greater in Phase IV than in Phase V, the total amount of 2,4-DNT volatilized from the soil surface 7.2 days after each rainfall event was approximately 15% greater in Phase V than in Phase IV. As discussed in section 3.1.2., higher soil moisture conditions allow for greater concentrations of 2,4-DNT in the

gas phase. If the gas phase 2,4-DNT is transported to the soil surface, there would be greater flux. In Phase V almost twice the amount of water was added to the soil as rainfall, and the amount of time for the soil to dry out, as evidenced by the uppermost WCR probe (Figure 5.2), also increased. Thus, for the same 7.2 day period following each rainfall event, the amount of water in the soil during Phase V was greater than that same time period of Phase IV. For reasons previously discussed, this moisture content condition accounts for the greater total 2,4-DNT flux in Phase V when compared to Phase IV.

On day 82, the plenum was changed again and the 2,4-DNT flux behaved as previously mentioned. Apparently the decrease in 2,4-DNT surface flux was not masked by desorption from the plenum and this concern was proven unfounded.

5.3. 2,4-DNT Soil Concentrations

Since 2,4-DNT was injected at a depth of 3.6 cm, it might seem that the 2,4-DNT concentrations should be highest at this depth in all bore holes. However, there are two reasons why this is not true. First, Phase II of Experiment II greatly increased the surface flux of water, so more 2,4-DNT could travel away from the injection point than in Experiment I. Furthermore, Phase III involved draining the soil column considerably by increasing the matric potential at the porous ceramic plate by 100 cm. This induced downward movement of the contaminant in the aqueous phase. However the dominant movement of 2,4-DNT in the column was upward, as evidenced by the highest 2,4-DNT concentrations existing above the injection point (Figure 5.5). For Experiment II,

discreet soil samples were taken in the same manner as experiment I and analyzed for their mass-2,4-DNT/mass wet soil. Again the 2,4-DNT concentrations appear to be highest at the center bore hole, the area most directly impacted by the injection of 2,4-DNT (Figure 5.5). Averaging the soil samples at each depth increment for bore holes 2,4,7, and 8 produces a single averaged concentration at a radial distance of 2.5 cm from the center of the column (Figure 5.6). As with Experiment I, it appeared that the data could be viewed as two-dimensional with an r and z coordinate system.

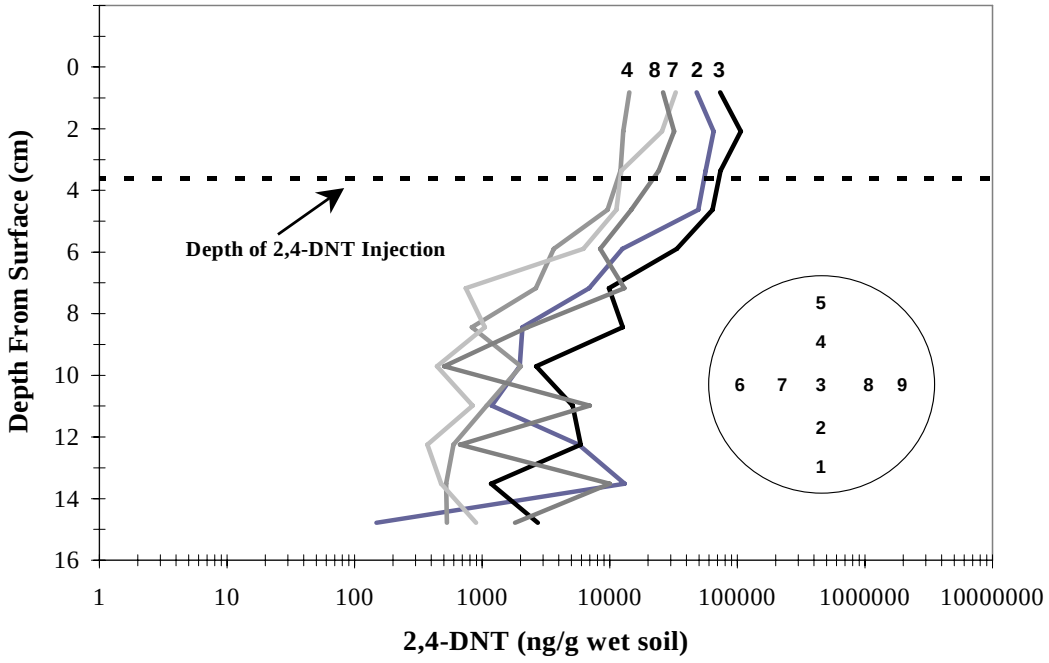

Figure 5.5. 2,4-DNT Soil Concentrations for Bore Holes 2,3,4,7 and 8 Experiment II

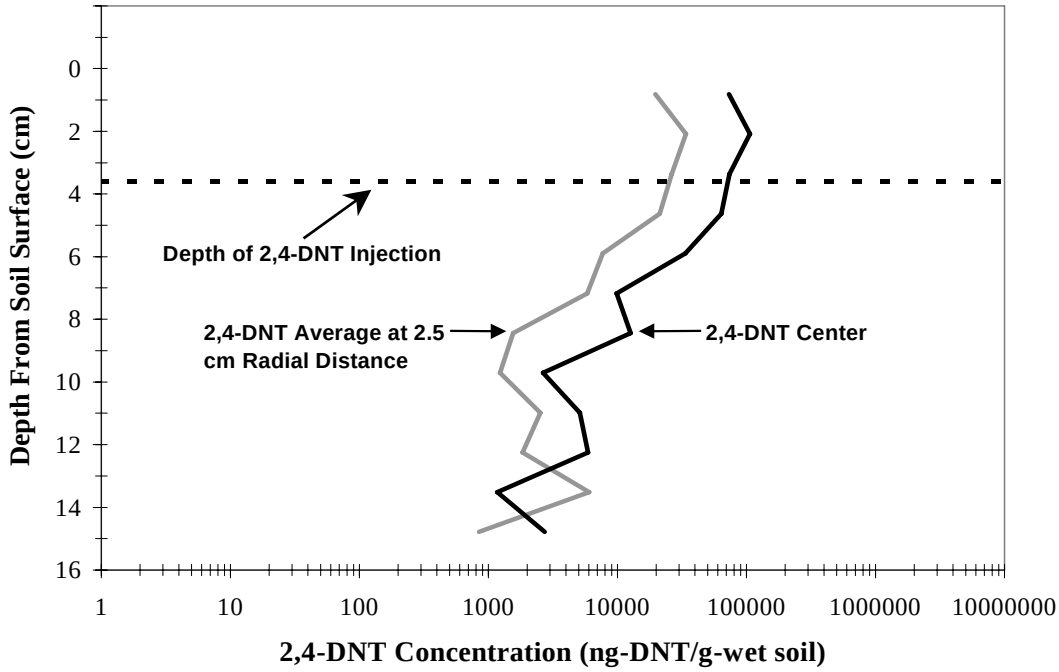

Figure 5.6. Avg. 2,4-DNT-Soil Concentrations at 2.5 cm Radial Distance and Column Center Experiment II

5.4. 2,4-DNT Mass Recovery Experiment II

All calculations performed for the 2,4-DNT mass recovery of Experiment II were exactly the same as for Experiment I. The only difference was that the data from Experiment II was used to calculate the mass recovery. The total mass injected into the column during the course of Experiment II was 19,300,000 ng-2,4-DNT. Using the estimations previously described the mass of 2,4-DNT residing in the soil column was 35,000,000 ng-2,4-DNT, and the amount of 2,4-DNT that was emitted from the soil surface was 5,000,000 ng. From these numbers and using Equation [4.3] it was determined that 208% of the mass injected was accounted for. Again, it is impossible to create mass. For the same reasons as previously described for Experiment I, this mass recovery can only be viewed as an approximation.

5.5. Data Model Comparison - Experiment II

The same model used to simulate the data from Experiment I was used to simulate the data from Experiment II, with the modification that T2TNT was changed to handle a non linear aqueous-solid distribution coefficient. The computer code was run with a boundary layer ratio of 0.5, and a Freundlich sorption isotherm with $C_s=1.7C_l^{0.82}$, Even with imperfections in the model present, the simulations produced by Stephen W. Webb of Sandia National Laboratories closely matched the data generated for Experiment II. Again, the data was modeled in a two dimensional system in r and z coordinates. Output was selected at z-values from 0 to 15 cm and at r-values of 0.0 and 2.9 cm to evaluate the performance of the computer code (Figure 5.7). The r value of 2.9 cm was chosen over 2.5 cm so that the simulations would roughly correlate with the outermost edge of the bore hole sample. The actual data collected from the soil column seems to correspond well to the simulation at depths between 0 and 5 cm. Below 5 cm from the surface, the predicted and measured values diverge, with the measured values being higher in concentration than those simulated with the model. One possible reason for this divergence is that it was difficult to discern if the samples taken below 5 cm were not contaminated with the sampling tube, or from soil or soil moisture that had been compressed into lower sampling intervals. Although the contamination would have had to be massive, it may have occurred. Since the main interest was to determine what would happen to the 2,4-DNT from the point of injection up to the surface, the model was deemed to have performed satisfactorily. In addition, since the samples from bore holes 2,4,7, and 8 were taken at a radial distance of 2.5 cm from the center of the column, the concentrations predicted by the model at 2.9 cm from the column center seem to be

reasonable, which was another indication that the model performed well.

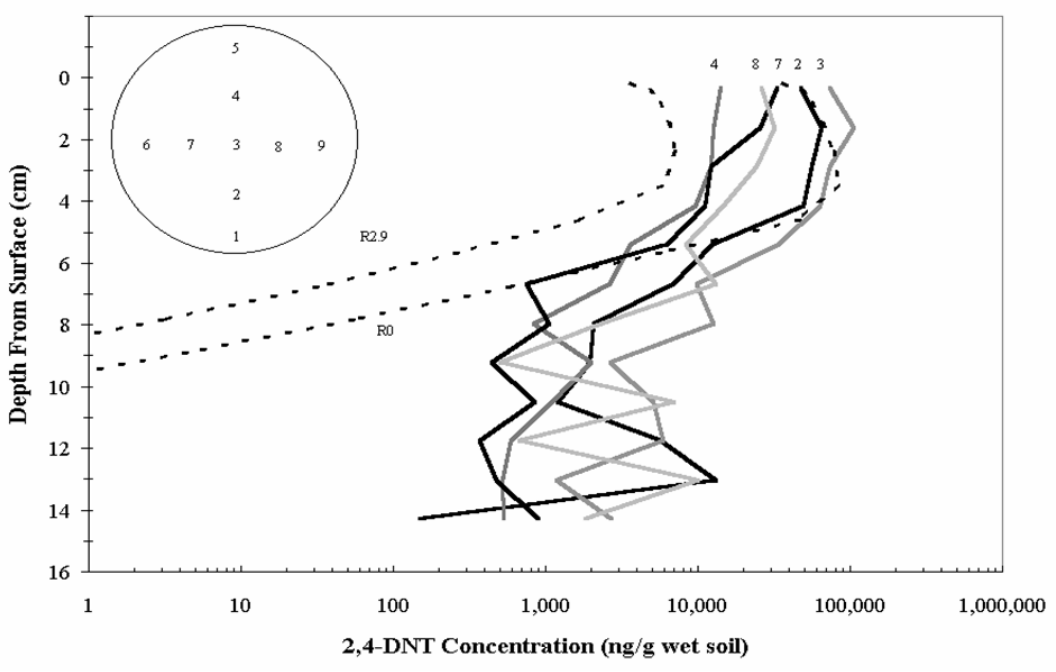

Figure 5.7. Data-Model Comparison for 2,4-DNT in Soil Column Experiment II

The model was also run to determine its ability to simulate the soil surface flux measured in the experiment (Figure 5.8). The simulation seems to have modeled the general shape of the surface flux curve well. Before day 38, T2TNT seems to have overpredicted the measured surface flux. This may be due to the uncertainty of surface soil water contents, and uncertainty in the aqueous solid distribution coefficient as described in section 4.5.

However, after day 38, the simulation seemed to predict the 2,4-DNT surface flux very well until day 70. The reason for such good correlation seems to be the calibration point for soil surface water content was measured on day 70. T2TNT also predicts the two wetting events fairly well. During the wetting phase of Experiment II, the model seems to overpredict the increase of 2,4-DNT surface flux. The uncertainty in data point

measurements was probably the cause for error in these instances, since the surface flux rose so quickly during these events that it was impossible to measure the initial spike of surface flux immediately following the rainfall event. During the drying portion following the rainfall events, the model overpredicted the 2,4-DNT surface flux. This was probably due, again to the uncertainty in soil surface water content.

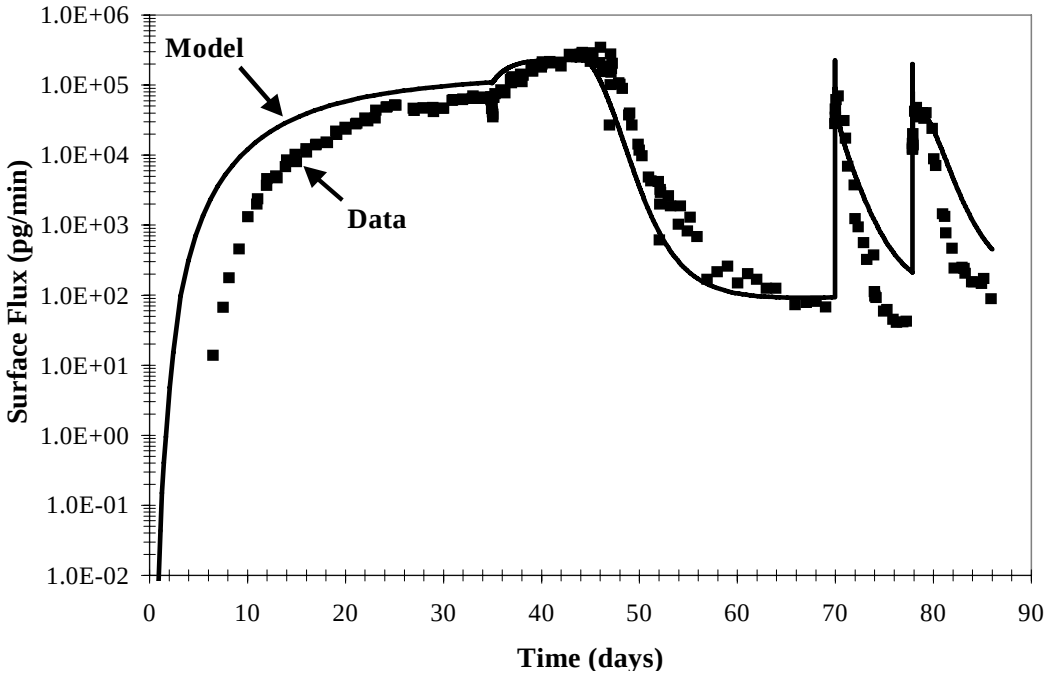

Figure 5.8. Data-Model Comparison 2,4-DNT Surface Flux Experiment II

6. CONCLUSIONS

The major goal of this experiment was to determine how great of an impact certain conditions would have on the soil surface flux of aqueous phase point source of 2,4-DNT. In an effort to do this, an instrumented soil column was built in which to conduct the experiment, a plenum-2,4-DNT sampling protocol was developed, and WCR probes were calibrated and used to measure moisture content in the soil-column. In addition, measurements of several soil properties were made as well as the K_d and K_d' distribution coefficients. Furthermore, the data generated in this series of experiments was used to calibrate a computer model by Stephen W. Webb at Sandia National Laboratories. Overall the experiments and modeling agreed reasonably well. The 2,4-DNT surface flux behaved as anticipated and also had good correlation with the model's predictions.

Specifically it was learned from these experiments that:

- At steady state boundary conditions, surface flux from a point source of 2,4-DNT will behave like a breakthrough curve for a contaminant rising from 0.0 to ~70,000 pg of 2,4-DNT per minute over the course of 35 days.

- Once the soil moisture drops below approximately 7.8 % volumetric, the 2,4-DNT surface flux will decrease exponentially, as predicted by K_d' partitioning theory. Although it was impossible to know the water content at the soil surface, except for the one direct measurement that was made at the beginning of Phase IV of Experiment II, drying of the soil surface to approximately 4% volumetric water content had the effect of dropping the 2,4-DNT surface flux from ~275,000 to 70 pg/min over 25 days.
- If the water evaporation rate increases from a soil surface with little to no change in the soil moisture content, then the 2,4-DNT soil surface flux will also increase. In Experiment II this increase occurred from ~70,000 to ~260,000 pg of 2,4-DNT per minute.
- When there is rainfall, followed by a period of drying, the 2,4-DNT surface flux will rapidly increase several orders of magnitude and then decrease as the soil dries again. In Experiment II the 2,4-DNT surface flux increased from ~70 to ~70,000 pg/min in six hours and then decreased to ~70 pg/min after 10 days during the first rainfall event. When the second rainfall event was attempted with a greater addition of water the 2,4-DNT Surface flux again rose from ~70 to ~ 50,000 pg/min.

6.1. Applications of Results

Since the impetus for conducting this research was to ultimately detect landmines, this research has some very important contributions to make to the de-mining effort worldwide. It is already known that the 50-200 g explosive charge of landmines contain from 0 to 0.5% 2,4-DNT (Phelan and Webb, 1997). This results in a source term of

anywhere from 0 to 10 g of 2,4-DNT in a typical landmine. In Experiments I and II, a total of 6.4E-3 and 1.9E-3 g of 2,4-DNT was injected, respectively. This mass is on the low end of what is typically found in a landmine. However, it is presently unknown how much of that 2,4-DNT will leak from a mine casing. Research is currently being conducted at Sandia National Laboratories (Albuquerque, NM) and the Cold Regions Research and Engineering Laboratory (Hanover, NH) to determine how much 2,4-DNT will leak out of several different types of anti-personnel mines.

These experiments have shown that the emissions of 2,4-DNT can be as low as the picogram/minute level (Figure 5.1). Although no detector has been developed specifically for the use of measuring 2,4-DNT, recent sensor developments include a detector capable of detecting a variety of nitroaromatic compounds (La Grone et al., 2000). In fact 2,4,6-trinitrotoluene has been detected at a level that would be comparable to 6.5 pg/min in the experiments presented here. If this sensor can be optimized for a similar magnitude detection of 2,4-DNT, then it seems almost certain that the detection of mines though their chemical signature is within grasp.

The findings presented here could be applied easily to a real world demining activity, once chemical detectors are adequately developed. It was found that rain following a period of drying would increase the 2,4-DNT signal by approximately three orders of magnitude. If a suspected mine field were doused with water from a water truck or water was dumped from a helicopter following a dry spell, fluxes of 2,4-DNT from a mine should increase significantly. This would provide an optimum window for detecting the

2,4-DNT signature emanating from a buried mine.

In addition, the experimental set-up employed in this series of experiments has never been used to study the behavior of herbicides and pesticides applied at the soil surface. Although Jury (1983, 1984 a,b,c) and Spencer and Cliath (1973) have all addressed the issue of semivolatile compound flux from a soil surface in detail, it is still interesting to note that this experimental set-up could be used to examine a number of these chemicals, and analyze their behavior in the sub-surface with realistic top and bottom boundary conditions.

6.2. Recommendations For Future Work

Although many of the boundary conditions pertinent to conditions in a landmine field were examined in this research, there are still several other conditions which could be examined to gain a more complete understanding. They are:

- Develop a procedure to mimic the effects of sunlight at the soil surface. Sunlight is known to photodegrade many organic compounds. It also has the effect of warming the soil surface. Both of these conditions could have an impact on the soil surface flux of 2,4-DNT.
- Conduct a similar experiment with variable wind speeds at the soil surface. Increased wind speed would have the effect of drying out the soil surface and therefore decreasing 2,4-DNT surface flux.
- Exactly determine the biological half-life of 2,4-DNT within the soil used for these

experiments. At present it is unknown.

- Conduct similar experiments with an actual landmine as the source of 2,4-DNT. This experiment, as of this writing, is currently underway at Sandia National Laboratories.
- Conduct a column K_d test to determine a value for the aqueous-solid distribution coefficient more suitable for conditions with the experimental set-up

REFERENCES CITED

1. 40 CFR 796, 1998. Code of Federal Regulations, Subpart C - Transport Processes, § 796.2750 Sediment and soil adsorption isotherm. U.S. Environmental Protection Agency.

2. Borchers, B., J.M.H. Hendrickx, B.S. Das, S.H. Hong. 2000. Enhancing Dielectric Constant Between Land Mines and the Soil Environment by Watering: Modeling, Design, and Experimental Results. In Detection and Remediation Technologies for Mines and Minelike Targets V. Edited by A. Dubey, J. Harvey, T. Broach, R. Dugan. Proceedings of SPIE Vol. 4038.

3. Fetter, C.W. 1999. *Contaminant Hydrogeology*. 2d ed. Upper Saddle River: Prentice Hall Inc.

4. Fuller, E.N., P.D. Schettler, J.C. Giddings. 1966. A New Method For Prediction of Binary Gas-Phase Diffusion Coefficients. *Industrial and Engineering Chemistry* 58, no. 5:19-27.

5. Gee, G.W., and J.W. Bauder. 1986. Particle Size Analysis. Chap. 9 in *Methods of Soil Analysis*. Edited by Arnold Klute. Madison, WI: American Society of Agronomy and Soil Science Society of America.

6. Heilman, M.D., D.L. Carter, and C.L. Gonzalez. 1965. The Ethylene Glycol Monoethyl Ether (EGME) Technique for Determining Soil-Surface Area. *Soil Science* 100:409-413.

7. Horton, R., P.J. Wierenga, D.R. Nielsen. 1982. A Rapid Technique for Obtaining Uniform Water Content Distributions in Unsaturated Soil Columns. *Soil Science* 133, no.6:397-99.

8. Jenkins, T.F., D.C. Leggett, T.A. Ranney. 1999. Vapor Signatures from Military Explosives. Special Report 99-21. Cold Regions Research and Engineering Laboratory, Hanover, New Hampshire.

9. Jury, W.A., W.F. Spencer, and W.J. Farmer. 1983. Behavior Assessment Model for Trace Organics in Soil: I. Model Description. *Journal of Environmental Quality* 12, no. 4:558-564

10. Jury, W.A., W.J. Farmer, and W.F. Spencer. 1984a. Behavior Assessment Model for Trace Organics in Soil: II. Chemical Classification and Parameter Sensitivity. *Journal of Environmental Quality* 13, no. 4:567-572.

11. Jury, W.A., W.F. Spencer, and W.J. Farmer. 1984b. Behavior Assessment Model for Trace Organics in Soil: III. Application of Screening Model. *Journal of Environmental Quality* 13, no. 4:573-579.

12. Jury, W.A., W.F. Spencer, and W.J. Farmer. 1984c. Behavior Assessment Model for Trace Organics in Soil: IV. Review of Experimental Evidence. *Journal of Environmental Quality* 13, no. 4:580-586.

13. Klute, Arnold. 1986. Water Retention: Laboratory Methods. Chap. 26 in Methods of Soil Analysis. Edited by Arnold Klute. Madison,WI: American Society of Agronomy and Soil Science Society of America.

14. La Grone, M., C. Cumming, M. Fisher, M. Fox, S. Jacob, D. Reust, M Rockley, E. Towers. 2000. Detection of Landmines by Amplified Fluorescence Quenching of Polymer Films: A Man-Portable Chemical Sniffer for Detection of Ultra-Trace Concentrations of Explosives Emanating from Landmines. In Detection and Remediation Technologies for Mines and Minelike Targets V. Edited by A. Dubey, J. Harvey, T. Broach, R. Dugan. Proceedings of SPIE Vol. 4038.

15. Ong, S.K. and L.W. Lion. 1991a. Mechanisms for Trichloroethylene Vapor Sorption onto Soil Minerals. *Journal of Environmental Quality* 20:180-188.

16. Ong, S.K. and L.W. Lion. 1991b. Effects of Soil Properties and Moisture on the Sorption of Trichloroethylene Vapor. *Water Resources Research* 25:29-36.

17. Ong, S.K., T.B. Culver, L.W. Lion, and C.A. Shoemaker. 1992. Effects of Soil Moisture and Physical-Chemical Properties of Organic Pollutants on Vapor-Phase Transport in the Vadose Zone. *Journal of Contaminant Hydrology* 11:273-290

18. Pella, P.A. 1977. Measurement of the Vapor Pressures of TNT, 2,4-DNT, 2,6-DNT and EGDN. *Journal of Chemical Thermodynamics* 9:301-305

19. Pennington, J.C., W.H. Patrick. 1990. Adsorption and Desorption of 2,4,6-Trinitrotoluene by Soils. *Journal of Environmental Quality* 19: 559-567.

20. Peterson, L.W., D.E. Rolston, P. Moldrup, and T. Yamagchi. 1994. Volatile Organic Vapor Diffusion and Adsorption in Soils. *Journal of Environmental Quality* 23:799-805.

21. Petersen, L.W., P. Moldrup, Y.H.El-Farhan, O.H. Jacobsen, T. Yamaguchi, and D.E. Rolston. 1995. The Effect of Moisture and Soil Texture on the Adsorption of Organic Vapors. *Journal of Environmental Quality* 24:752-759.

22. Petersen, L.W., Y.H. El-Farhan, P. Moldrup, D.E. Rolston, and T. Yamaguchi. 1996. Transient Diffusion, Adsorption, and Emission of Volatile Organic Vapors in Soils with Fluctuating Low Water Contents. *Journal of Environmental Quality* 25:1054-1063.

23. Phelan, J.M., and S.W. Webb. 1997. Environmental Fate and Transport of Chemical Signatures from Buried Landmines - Screening Model Formulation and Initial Simulations. Report SAND97-1426. Sandia National Laboratories, Albuquerque, NM.

24. Phelan, J.M., S.W. Webb, P.J. Rodacy, J.L. Barnett, K. Pruess, S. Finsterle, M. Cal, and M. Gozdor. 1999. Environmental Impacts to the Chemical Signature Emanating from Buried Unexploded Ordnance. FY '99 Interim Technical Report for SERDP Project 1094. Sandia National Laboratories, Albuquerque, NM.

25. Phelan, J.M and J.L. Barnett. 2000. Solubility of 2,4-Dintrotoluene and 2,4,6-Trinitrotoluene in Water. Journal of Chemical and Engineering Data. Submitted November 8, 2000.

26. Phelan, J.M., M. Gozdor, S.W. Webb, M. Cal. 2000. Laboratory Data and Model Comparisons of the Transport of Chemical Signatures From Buried Landmines/UXO. Proceedings of the SPIE 14th Annual International Symposium on Aerospace/Defense Sensing, Simulation and Controls, Detection and Remediation Technologies for Mines and Minelike Targets V, April 24-28, 2000, Orlando, FL.

27. Rhoades, J.D. 1986. Electrical Conductivities of Soils. Chap. 14 in *Methods of Soil Analysis*. Edited by Arnold Klute. Madison, WI: American Society of Agronomy and Soil Science Society of America.

28. Seinfeld, J.H. and Pandis, S.N., *Atmospheric Chemistry and Physics*, Wiley-Interscience, 1999.

29. Spencer, W.F. and M.M. Cliath. 1973. Pesticide Volatilization as Related to Water Loss from Soil. *Journal of Environmental Quality* 2, no. 2:284-289.

30. Spencer, W.F., M.M. Cliath, W.A. Jury, Lian-Zhong Zhang. 1988. Volatilization of Organic Chemicals from Soil as Related to Their Henry's Law Constants. J. Environmental Quality, Vol 17, no.3:504-509.

31. U.S. Environmental Protection Agency. 1986. *SW846-9060 Total Organic Carbon.* Washington D.C.: GPO.

32. U.S. Environmental Protection Agency. 1994. *SW846-8330 Nitroaromatics and Nitroamines by High Performance Liquid Chromatography (HPLC)*. Washington D.C.: GPO.

33. U.S. Environmental Protection Agency. 1998. *SW846-8095 (proposed) Explosives by GC-ECD*. Washington D.C.: GPO.

34. U.S. Occupational Safety and Health Administration. 1983. *Method no. 44 2,4-Dinitrotoluene (2,4-DNT) 2,4,6-Trinitrotoluene*. Salt Lake City: OSHA.

35. Webb, S.W., K. Pruess, J.M. Phelan, and S.A. Finsterle, 1999. Development of a Mechanistic Model for the Movement of Chemical Signatures from Buried Landmines/UXO. Proceedings of the SPIE 13th Annual International Symposium on Aerospace/Defense Sensing, Simulation and Controls, Detection and Remediation Technologies for Mines and Minelike Targets IV, April 5-9, 1999, Orlando, FL.

.